Saudi Journal of Biological Sciences 28 (2021) 1401–1416

Contents lists available at ScienceDirect

Saudi Journal of Biological Sciences

journal homepage: www.sciencedirect.com

Original article

Optimization of growing conditions for pigments production from microalga *Navicula incerta* using response surface methodology and its antioxidant capacity

Ricardo Iván González-Vega [a], José Luis Cárdenas-López [a], José Antonio López-Elías [a], Saúl Ruiz-Cruz [b], Aline Reyes-Díaz [a], Liliana Maribel Perez-Perez [a], Francisco Javier Cinco-Moroyoqui [a], Ramón Enrique Robles-Zepeda [a], Jesús Borboa-Flores [a], Carmen Lizette Del-Toro-Sánchez [a,*]

[a] Universidad de Sonora, Blvd. Luis Encinas y Rosales SN, Centro, 83000 Hermosillo, Sonora, Mexico
[b] Instituto Tecnológico de Sonora, 5 de Febrero 818 Sur, Centro, 85000 Ciudad Obregón, Sonora, Mexico

ARTICLE INFO

Article history:
Received 28 August 2020
Revised 18 November 2020
Accepted 24 November 2020
Available online 1 December 2020

Keywords:
Optimization
Response surface methodology
Navicula incerta
Pigment production
Antioxidant capacity
Chemoprevention

ABSTRACT

Navicula incerta is a marine microalga distributed in *Baja California, México,* commonly used in aquaculture nutrition, and has been extended to human food, biomedical, and pharmaceutical industries due to its high biological activity. Therefore, the study aimed to optimize culture conditions to produce antioxidant pigments. A central composite experimental design and response surface methodology (RSM) was employed to analyze the best culture conditions. The medium (nitrogen-deficient concentrations), salinity (PSU = Practical Salinity Unity [g/kg]), age of culture (days), and solvent extraction (ethanol, methanol, and acetone) were the factors used for the experiment. Chlorophyll *a* (Chl a) and total carotenoids (T-Car), determined spectroscopically, were used as the response variables. The antioxidant capacity was evaluated by $DPPH^{\bullet}$ and $ABTS^{\bullet+}$ radical inhibition, FRAP, and anti-hemolytic activity. According to the overlay plots, the optimum growth conditions for Chl *a* and T-Car production were the following conditions: medium = 0.44 mol·L^{-1} of $NaNO_3$, salinity = 40 PSU, age of culture: 3.5 days, and solvent = methanol. The pigment extracts obtained in these optimized conditions had high antioxidant activity in $ABTS^{\bullet+}$ (86.2–92.1% of inhibition) and anti-hemolytic activity (81.8–96.7% of hemolysis inhibition). Low inhibition (33–35%) was observed in $DPPH^{\bullet}$. The highest value of FRAP (766.03 ± 16.62 μmol TE/g) was observed in the acetonic extract. The results demonstrated that RSM could obtain an extract with high antioxidant capacity with potential applications in the biomedical and pharmaceutical industry, which encourages the use of natural resources for chemoprevention of chronic-degenerative pathologies.

Abbreviations: CP, crude protein; CL, crude lipid; RSM, response surface methodology; Chl *a*, chlorophyll *a*; T-Car, total carotenoids; PSU, salinity expressed as practical salinity unity (g/kg); CCD, central composite design; CICECE, Centro de Investigación Científica y de Educación Superior de Ensenada; AOAC, Association of Official Analytical Chemists; DOE, design of experiment; ANOVA, analysis of variance; FRAP, ferric reducing antioxidant power; DPPH, 1,1-diphenyl-2-picrylhydrazyl; ABTS, 2,2′-azinobis (3-ethylbenzothiazolin)-6-sulfonic acid; AAPH, (2,2′-azobis-[2-methylpropionamidine]); RBC, red blood cells; EDTA, ethylenediaminetetraacetic; AOX, antioxidant; TE, trolox equivalent; IC_{50}, Concentration mean inhibitory; SET, single electron transfer; HAT, hydrogen atom transfer.

* Corresponding author.
E-mail address: carmen.deltoro@unison.mx (C.L. Del-Toro-Sánchez).

Peer review under responsibility of King Saud University.

Production and hosting by Elsevier

https://doi.org/10.1016/j.sjbs.2020.11.076
1319-562X/

1. Introduction

The diatom *Navicula incerta* is the main organic matter producer in aquaculture for use as food for various marine species (Lee et al., 2006; Fimbres-Olivarría et al., 2016). It is also used in biomedical and pharmaceutical areas due to its bioactive compounds (Richmond, 2004). Light, irradiance, pH, CO_2, temperature, salinity, and nutrient availability (Lu and Zhang, 2000; Masojídek et al. 2000; Beardall et al., 2001; Lu and Vonshak, 2002) are the main factors involved in the development of microalgae (Markou et al., 2012). The modification of culture medium directly impacts its reproduction, growth, and metabolic cycles (Beardall et al. 2001), but salinity and nitrogen-deficiency are some of the most critical environmental factors for biomass and pigment production (Schubert et al., 1993; Kraȁbs and Buȁchel, 2011). The microalgae exposed to these factors present physiological changes in metabolite content (Krell et al., 2007; Kumar et al., 2010) and photosynthetic efficiency (Rijstenbil, 2005). The photosynthetic pigment composition and relative concentration are highly related to development under these factors (salinity and low-nitrogen medium) (Schubert et al., 1993, Liang et al., 2014). On the other hand, carotenoid concentration has been observed to increase in a low-nitrogen medium. However, there is a lower concentration of cells with higher carotenoids content, mainly carotenes (López-Elías et al., 2013; García-Morales et al., 2020). These physiological changes have been observed in diatoms (Radchenko and Il'yash, 2006; Kraȁbs and Buȁchel, 2011), increasing the synthesis of photosynthetic pigments. These facts indicate that *N. incerta* could be a good source of antioxidant compounds that could be applied in the functional food field with benefits to human health due to its biological activity (Kyong-Hwa et al., 2011), such as the antioxidant capacity, and this characteristic is important for consumption in the human food market.

A further increase in the photosynthetic pigments could be obtained by optimizing the growing conditions that better stimulate the synthesis of carotenoids and chlorophylls. For this, alternative methods are being used to maximize the production of these compounds. The statistical optimization process arises from an experimental perspective to establish the best microalgae culture conditions (Xin et al., 2010; Calderon et al., 2016). Optimization is essential for the aquaculture industry because it reduces costs and time for production. It is also used to select the best criterion from a set of factors that use different statistical methodologies (Athmouni et al., 2017; Li et al., 2017). Response surface methodology (RSM) is used to obtain the maximum optimized level of important factors through screening or factorial designs, mainly if the curvature of response is found (Bezerra et al., 2008; Saurabh et al., 2016). Unlike factorial designs, the curvature is obtained by second-order polynomial equations of the factors present in the RSM models, with changes in the variables that affect curvature, getting in that way a complete scan of the responses studied (Chih Wei et al., 2017). This quadratic model fits the central composite design (CCD), used in a sequential experiment with an adequately planned factorial design. These advanced statistical techniques were used to optimize the synthesis of antioxidant compounds, improve their performance, and their antioxidant activity (Laokuldilok et al., 2016).

The primary metabolites present in microalgae are photosynthetic pigments such as chlorophylls and carotenoids. They can donate electrons to stabilize reactive oxygen species due to the presence of a chromophore, which consists mainly of a chain of conjugated double bonds easily oxidizable, responsible for a variety of colors (yellow, orange, and red, among others). The pigments (chlorophylls and carotenoids) have a high free radical-scavenging capacity related to preventing of chronic degenerative diseases (Richmond, 2004; Gagez et al., 2012). Currently, the study of microalgae pigments has increased considerably due to their high biological activity. β-carotene, astaxanthin, and fucoxanthin are the main pigments present in different microalgae (*Dunaliella* sp, *Cyanophora paradoxa, Tetraselmis chuii*, and *Haematococcus pluvialis*) with high antioxidant activity (Gagez et al., 2012; Li et al., 2017; Widowati et al., 2017). One of the main potential antioxidants is astaxanthin from *Haematococcus pluvialis,* which considerably reduces ROS in melanocytes caused by UV radiation, preventing the appearance of skin cancer. In recent studies, peptides and stigmasterol from *N. incerta,* have shown strong biological potential. They act as scavengers of superoxide and hydroxyl radicals and significantly reduce liver cancer tumors (Kyong-Hwa et al., 2011). However, photosynthetic pigments have not been studied yet in *N. incerta*. This study is the first report to describe a pigment and its antioxidant activity. Besides, the use of advanced optimization tools in health could give added value to research. Therefore, this study aimed to optimize growing conditions for pigment production (carotenoids and chlorophylls) from microalga *Navicula incerta* at different culture conditions (salinity and low-nitrogen medium) using response surface methodology and antioxidant capacity, stimulating better carotenoids and chlorophylls synthesis by salinity and low-nitrogen medium as environmental factors.

2. Materials and methods

2.1. Microalgae strain

The diatom *N. incerta* was obtained from *Centro de Investigación Científica y de Educación Superior de Ensenada (CICECE), Baja California, México*. The diatom was cultivated at different salinities (25, 35, 45, and 55 PSU = Practical Salinity Unity, that are units to characterize the concentration of dissolved mineral salts (g) in a body of water (kg)) and nitrogen-deficient concentrations (0.22, 0.44, and 0.88 mol·L^{-1} of $NaNO_3$) in 1L flasks with a 700 mL volume of culture. The culture medium was kept at pH 7.0 with constant aeration for better homogenization. Continuous light (24 h) was applied by light-emitting diode lamps (LED) electronically regulated for handling the desired intensity. White wavelength (400–750 nm) was used to an intensity of 100 μmol photon/m^2/sec. A quantic spherical sensor Li-Cor 193SA was used to measure irradiance and wavelength. The F/2 (0.88 mol·L^{-1} of $NaNO_3$ at 35 PSU) medium from Guillard and Ryther (1962) was employed as a control medium, composed mainly of nitrates (75 g L^{-1}), phosphates (5 g L^{-1}), silicates (30 g L^{-1}), trace metals (22.81 g 100 mL^{-1}) and vitamins (1.1 g L^{-1}). This medium is the most used for microalgae culture in aquaculture. To analyze the growth kinetics, the experimental culture media were subjected to stress conditions (nitrogen deficiency and different salinities): F/2 (0.88 mol·L-1 of $NaNO_3$ at 25, 45, and 55 PSU), F/4 (0.44 mol·L^{-1} of $NaNO_3$ at 25, 35, 45, and 55 PSU), and F/8 (0.22 mol·L^{-1} of $NaNO_3$ at 25, 35, 45, and 55 PSU).

2.2. Effect of culture conditions on biomass production

The effect of different variables on culture conditions was observed. The results obtained from growth kinetics, biomass yields, and chemical composition showed the behavior under cellular stress conditions for biomass production.

2.2.1. Growth kinetics

Growth kinetics was determined every 24 h for six days by cell concentration using a Neubauer chamber (0.1 mm deep) in an optical microscope (Olympus CX43 microscopy Europe). The data

generated were analyzed with the following equation (1) (Richmond, 2004):

$$\left(\#\frac{cells}{8}\right) * 10000 = \frac{\#Cells}{mL} \quad (1)$$

Mean growth rates (μ) were estimated based on the following formula: mean growth rate μ = Log_2B_n- $Log_2B_0/(t_n\text{-}t_0)$. Where B_n and B_0 are the cell concentration determined on times t_n and t_0. The initial cell concentration was 70 $x10^3$ cell·mL^{-1} for all experiments.

2.2.2. Biomass yields and chemical composition

Biomass yield was determined by weighing the total cultivated biomass collected after lyophilization (Yamato Scientific CO., LTD. Japan). First, the biomass was harvested at the end of the exponential phase and washed with sodium formate to remove the salt for each treatment tested. Later, the entire culture was lyophilized. The chemical composition of the biomass microalgal was evaluated at the end of the exponential phase. The crude protein (CP) was determined by the copper catalyst micro-Kjeldahl nitrogen (AOAC, 2000; method 955.04). The nitrogen-to-protein conversion factor used to estimate the percentage of CP was 4.78, as suggested by Lourenço et al. (2004). For determination of the lipid concentration, an amount of 0.5 g of microalgal sample was used. The crude lipid (CL) was extracted under a Soxhlet automated system device (model 2050, FOSS North America, USA) with 33 × 80-mm extraction thimbles by ether (100 mL) at 150 °C for 82 min. In this case, the extraction was finished after 4 extraction cycles have been completed (approximately 90 min). Finally, CL content was determined gravimetrically after oven-drying (105 °C) the lipid extract (AOAC 1997, method 920.85). For ash determination, the sample (1 g) was burned in a muffle at 550 °C for 24 h. The ash content (AOAC 2000, method 920.153) was estimated as the difference between the dry weight and the ash. The carbohydrate content was estimated by difference, as suggested by Tibbetts et al. (2014).

2.3. Generation of the optimization matrix and model prediction performance

The optimization matrix and model prediction were generated using the statistical package JMP version 9.0.1 for Mac (SAS Institute Inc., NC, U.S.A). Here, the statistical tool DOE (design of experiments) was applied to improve the pigment production process and reduce its variability to identify the response variables changes through a central composite experimental design. Hence, this section analyzed the optimum processing conditions that provide the best pigment production (Sorokin, 1973; Agcam et al., 2017).

2.3.1. Experimental design and statistical optimization

A central composite design (CCD) of four factors and three levels for each factor was used. The independent variables were culture medium (0.22–0.88 mol·$L^{-1}$of $NaNO_3$), salinity (25–55 PSU [g/kg]), age of culture (1–6 days), and solvent type (acetone, methanol, and ethanol). The response variables in the culture condition were chlorophyll *a* (Chl *a*) and total carotenoids (T-Car). This experimental design will define which experiments should be carried out in the experimental region studied (Hanrahan and Lu, 2006). The control was performed with the following condition: medium = 0.88 mol·$L^{-1}$of N, salinity = 35 (PSU), and age of culture (harvested at the end of the exponential phase, 3.5 days). This methodology is based on the experiment (DOE) to carry on optimize growing conditions for pigment production. The CCD was based on second-order polynomial equations for each response. The results were based on the following equation (2) (Almeida et al., 2008; Altan et al., 2008).

$$Y = \beta_0 \sum_{i=1}^{k} \beta_i X_i + \sum_{i=1}^{k} \beta_{ii} X_{ii}^2 + \sum_{i}^{k-1} \sum_{j}^{k} \beta_{ij} X_i X_j + e_i \quad (2)$$

where Y represents the response function; β_0 is a constant coefficient (origin); β_i, β_{ii}, and β_{ij} are the coefficients of the linear equation; k is a number of variables and e_i is the experimental error or residual.

The CCD drew an optimization matrix, where all data obtained from the response variables were recorded. Also, as part of the statistical support, an analysis of variance (ANOVA) was performed with a confidence level of 95%. A backward regression analysis was applied to remove non-significant factors ($p > 0.05$) from the second-order polynomial equation. Later, the final predictive model presented an equation for each response variable (Altan et al., 2008).

2.3.2. Response surface methodology (RSM)

RSM was applied to determine the best conditions for pigment production with response variables chlorophyll *a* and total carotenoids to optimize the process (Myers et al., 2009). Superposition surface methodology was applied to achieve the optimization technique and generate a response surface plot. The optimization matrix and response surface plot were generated using JMP version 9.0.1 for Mac (SAS Institute Inc., NC, U.S.A) statistical package. This methodology was used to define the minimum and maximum limits and the experimental variables studied. Validation of the optimization model was performed according to the estimated processing values obtained by CCD. The optimized treatment was used to perform the antioxidant capacity assays of three different extracts of *N. incerta*.

2.3.3. Pigment extraction and quantification of N. Incerta

The biomass was harvested under the specific conditions obtained by the optimization matrix. Subsequently, methanolic, acetonic, and ethanolic pigment extracts were obtained using 0.1 g of the dry weight of lyophilized biomass and resuspended in 10 mL of the solvent. The pigment extraction was assisted by ultrasonic pulses (Generator ultrasonic pulses Branson Digital Sonifier Qsonica, LLC. E.U.A.). These were done at 400 w, 500 mHz, and 15 s per pulse at an amplitude of 30%, and then it was placed in constant agitation for 1 h in darkness. The supernatant was recovered by centrifugation at 4000 × *g* for 20 min at 4 °C. Later, it was concentrated in a rotary evaporator (Laborata 4000 Heidolph. Germany) at 45–50 °C. The resulting extract was re-suspended in each solvent (acetone, methanol, and ethanol) at the final concentration of 10 μg of pigment·mL^{-1}. The absorption spectral of 300 μL of each extract was measured in a 96-well microplate reader (UV–Vis spectrophotometer, Thermo Fisher Scientific Inc. Multiskan GO, NY, USA). The quantification (μg/mL) of Chl *a* and T-Car of *N. incerta* extracts (acetonic, methanolic, and ethanolic) was determined according to Jeffrey and Humphrey (1975) and Lichtendthaler and Welburn (1983) using the following equations (*Eq* (3)):

Acetone

$$Chla = 11.47A_{664} - 0.64A_{630}$$

$$T - Car = (1000A_{470} - 2.276C_a - 81.4C_b)/227$$

Methanol

$$C_a = 15.65A_{666} - 7.34A_{653}$$

$$C_b = 27.05A_{653} - 11.21A_{666}$$

$$C_{x+c} = (1000A_{470} - 2.86C_a - 129.2C_b)/221$$

Ethanol

$$C_a = 13.95A_{665} - 6.88A_{649}$$

$$C_b = 24.46A_{649} - 7.32A_{665}$$

$$C_{x+c} = (1000A_{470} - 2.05C_a - 114.8C_b)/245 \quad (3)$$

where, Chl*a* = chlorophyll *a*; T – Car = total carotenoids and *A* = absorbance.

2.4. Antioxidant capacity study

The antioxidant capacity assay was determined in methanolic, acetonic, and ethanolic pigment extracts, adjusting their solids to a final concentration of 780 μg of pigment·mL^{-1}. From these extracts the measurements of Ferric reducing antioxidant power (FRAP); 1,1-diphenyl-2-picrylhydrazyl (DPPH); 2,2′-azinobis (3-et hylbenzothiazolin)-6-sulfonic acid (ABTS), and Anti-hemolytic assays were made.

2.4.1. FRAP assay

The reducing power of pigment was determined using the FRAP assay described by Benzie and Strain (1996), with some modifications. The stock solutions were sodium acetate buffer (300 mM, pH 3.6), $FeCl_3$ (20 mM) and TPTZ (2,4,6-tripyridyl-s-triazine) solution (10 mM) in HCl (40 mM). The FRAP working solution was prepared in a relation 10:1:1 (Buffer:$FeCl_3$:TPTZ). A volume of 20 μL of each extract was combined with a 280 μL FRAP solution and placed in a microplate reader (Thermo Fisher Scientific Inc. Multiskan GO, NY, USA). The increase in absorbance at 638 nm was monitored every 10 min for 40 min. A Trolox́s curve was made, and the results were expressed as μmol TE/g of dry sample. Trolox (antioxidant standard) is a synthetic compound similar to vitamin E that preserves antioxidant capacity. It is commonly used in biochemical applications to reduce oxidative stress. Trolox equivalent antioxidant capacity is an average of the Trolox-based antioxidant power measured in units called Trolox equivalents. These units help to understand the antioxidant capacity of an unknown sample.

2.4.2. DPPH free radical scavenging activity

The DPPH· free radical was prepared in methanol (6×10^{-5} mol·L^{-1}), and an aliquot of 200 μL of this solution was combined with 20 μL of each pigment extract. The decrease in absorbance was determined at 515 nm for 30 min under the darkness. All determinations were carried out in triplicate. The results were reported as % of inhibition according to the equation (4). Additionally, the half-maximal inhibitory concentration (IC_{50}) was obtained (Brand-Williams et al., 1995).

$$\%\text{ofInhibition} = \left[1 - \frac{A_i - A_s}{A_c}\right] \times 100 \quad (4)$$

where, A_i is the absorbance of the extract mixed with DPPH· radical, A_s is the absorbance of the extract without radical, and A_c is the absorbance of the control.

2.4.3. ABTS free radical scavenging activity

The preformed radical monocation of ABTS$^{\bullet+}$ was generated according to Re et al. (1999). ABTS salt was weighed (19.3 mg) and dissolved in distilled water (5 mL). An amount of 88 μL from a solution of $K_2S_2O_8$ (0.0378 g/mL) was added to ABTS solution and leaving the mixture for 12 h at room temperature in the dark. The ABTS$^{\bullet+}$ solution was diluted with ethanol to an absorbance of 0.700 ± 0.05 at 734 nm for measurements. Afterward, 270 μL of the free radical solution was combined with 20 μL of each pigment extract. The absorbance was measured at 734 nm after 30 min of incubation at room temperature in the dark. Antioxidant activity, expressed as % of inhibition, was calculated using equation (4). Moreover, the half-maximal inhibitory concentration (IC_{50}) was obtained.

2.4.4. Anti-hemolytic activity

Before performing the anti-hemolytic activity, it is necessary to do a Venipuncture and arrangement of red blood cells (RBC) suspension. All processes using human blood were performed following the Mexican (NOM-253-SSA1-2012) and international (FDA: CFR - Code of Federal Regulations Title 21, part 640 Additional Standards for human blood and blood product, Support. B Red blood cells, Sec. 640.14 Testing the blood [21CFR640.14]) regulations. The laboratory where the sample was treated is accredited by ISO-IEC 17,025 (NMX-EC-17025) and ISO 15,189 elaborated by technical committee ISO/TC 212 (Clinical Laboratory Testing and In vitro Diagnostic Systems) taking as reference ISO/IEC 17,025 and ISO 9001. The erythrocytes were collected from healthy adult volunteers of 28–31 years old with prior consent obtaining each onés informed consent and using RBC with the venipuncture technique using a sterile vial containing anticoagulant (EDTA). The erythrocyte suspension was prepared at 10%. The suspension was centrifuged at 2000 × *g* for 10 min and washed three times with isotonic solution. RBC suspension was used to evaluate the anti-hemolytic activity and protective effect from extracts of *N. incerta*. Therefore, the experiments with erythrocytes are used as a cellular model and do not focus on the volunteers as an object of study.

To perform anti-hemolytic activity, firstly the hemolysis was induced by AAPH (2,2′-azobis-[2-methylpropionamidine]) radical according to the methodology of Lu et al. (2010) with some modifications. The globular package was separated from the plasma by centrifugation at 2000 × *g* for 10 min at 4 °C. The erythrocytes were washed three times with phosphate-buffered saline (PBS) pH 7.4. Afterward, a suspension of erythrocytes was prepared in PBS with a ratio of 5:95 (v/v). A mixture containing 100 μL of the erythrocytes, 100 μL of the AAPH radical and 100 μL of each extract (780 μg of pigment·mL^{-1}) was incubated at 37 °C for 3 h with continuous shaking (30 rpm). Subsequently, 1 mL of PBS was added and centrifuged at 2000 × *g* for 10 min at 4 °C. Suspension of erythrocyte and AAPH with erythrocytes were taken as controls. The supernatant was read at 540 nm on a 96-well microplate. The half maximal-inhibitory concentration (IC_{50}) was determined following Lu et al. (2010) procedure. The percentage of hemolysis inhibition (% HI) was obtained from the equation (5):

$$\%HI = \left(\frac{\text{AAPH1} - \text{HS}}{\text{AAPH1}}\right)x100 \quad (5)$$

where $AAPH_1$ is the optical density of the hemolysis caused per radical AAPH, and HS is the optical density of the hemolysis inhibition by each treatment.

The morphological change of RBC and protective effect of the pigment extracts was assessed by optical microscopy. This evaluation is performed after anti-hemolytic activity. The samples were taken immediately after reading the supernatant to obtain the percentage of hemolysis inhibition. The supernatant of the erythrocyte suspension was discarded after reading. The pellet (the globular package) was re-suspended at 50 μL of fresh plasma. Afterward, a drop of the treated blood samples was spread on a slide to create a single RBC film layer. Then, to observe the damage at the cellular membrane, the samples were stained with *Wright stain*. Later, the morphological changes were observed at 100x with an Eclipse FN1 microscope and capture in an image software NIS-Elements F. The result was compared with different controls: healthy erythrocytes, healthy erythrocytes with radical AAPH (v/v) and autoimmune hemolytic anemia were kindly provided by the Hematology

Laboratory of Biological Sciences Department from the University of Sonora, Mexico.

2.5. Statistical analysis

The experimental results were expressed as means ± standard deviation (n < 3). The two-way ANOVA was applied to evaluate the significant differences (Tukey post hoc test at a confidence level of $P < 0.05$) between different chemical composition variables. The CCD matrix and response surface plots were generated using JMP version 9.0.1 for Mac (SAS Institute Inc., NC, U.S.A). One-way ANOVA was applied to evaluate the significant differences at a $p < 0.05$ (Tukey test) confidence level by the antioxidant activity. Linear regression was used to measure the percentage of inhibition for the antioxidant activity.

3. Results

3.1. Growth kinetics

Fig. 1 shows the typical growth kinetic by the effect of the different factors and their respective levels. *N. incerta* shows a sigmoidal behavior in the different treatments, responding favorably to its growth (Fig. 1A, B, and C). In F/2 (Fig. 1A), F/4 (Fig. 1B), and F/8 (Fig. 1C) medium, the highest growth was found in the most saline medium (55 PSU), reaching its maximum cell density at 4, 5, and 3 days, respectively. The order of the mediums with maxi-

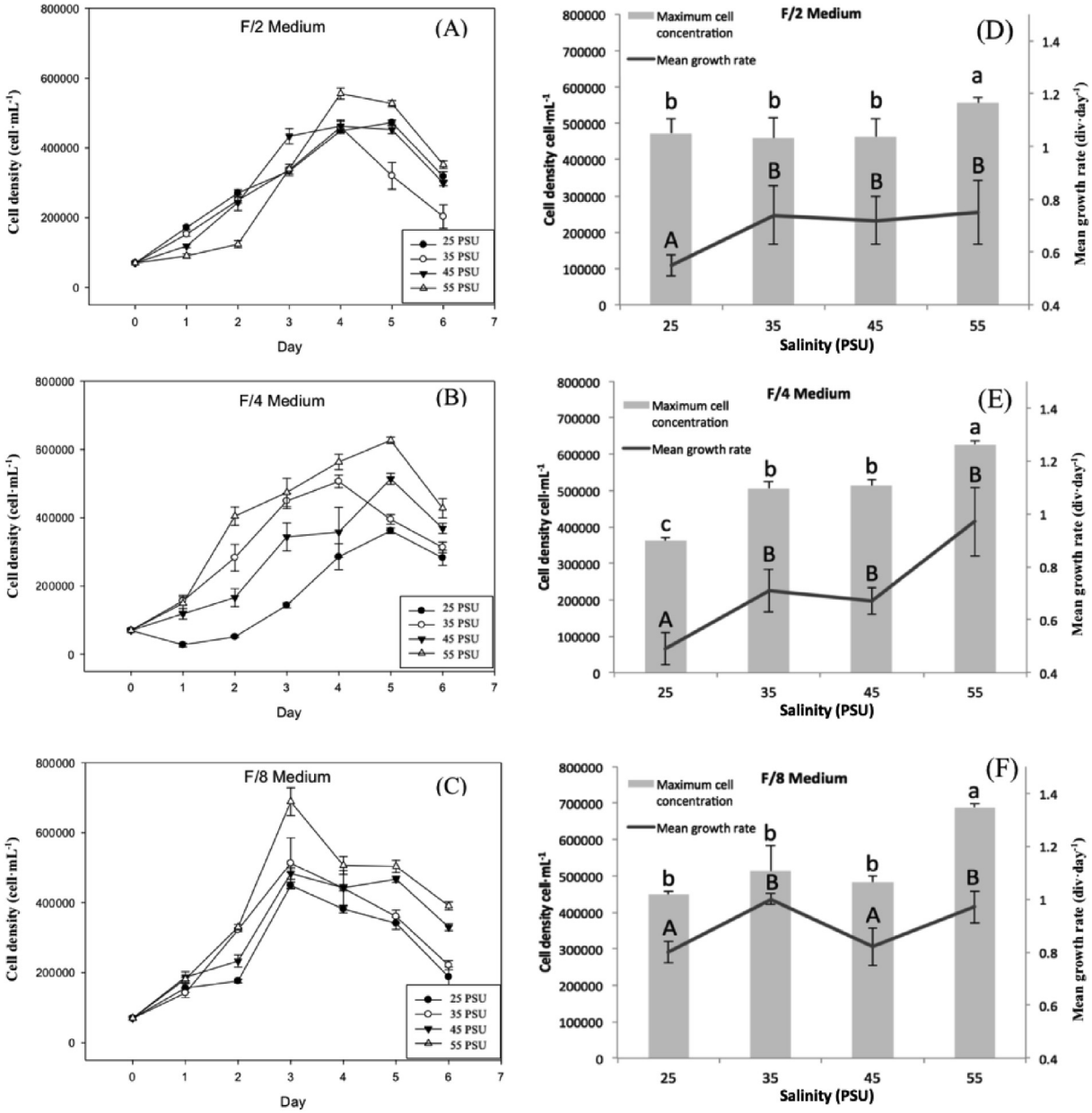

Fig. 1. Effect of different nitrogen-limited concentrations medium and salinity level on growth kinetic, cell density, and growth rate of *N. incerta*. (A) Growth kinetic of *N. incerta* in medium F/2 (0.88 mol·L^{-1} of N), (B) in medium F/4 (0.44 mol·L^{-1} of N), (C) in medium F/8 (0.22 mol·L^{-1} of N). (D) Maximum cell concentration and growth rate of *N. incerta* in medium F/2 (0.88 mol·L^{-1} of N). (E), in medium F/4 (0.44 mol·L^{-1} of N), (F) in medium F/8 (0.22 mol·L^{-1} of N). PSU = Practical Salinities Unity (g of dissolved salts/kg of water). The maximum cell concentration considered in D, E and F was for F/2 (day 4), F/4 (day 5), and F/8 (day 3), where these data correspond at the maximum increase during the growth period for each case. Each data point corresponds to the average of 3 determinations (n ≥ 3), and error bars correspond to the standard deviation.

mum cell density was F/8 > F/4 > F/2. The cell concentration of 688,750 ± 29,509 cell·mL^{-1} was the highest obtained by the F/8 medium. The main growth rate in F/2 (Fig. 1D) and F/4 (Fig. 1E) medium did not significantly differ at 35, 45, and 55 PSU. While in the F/8 (Fig. 1F) medium, presented main growth rate of 1 div day^{-1} at 35 and 55 PSU., resulting in a rapid replication rate.

3.2. Biomass yields and chemical composition

The biomass yields increase at hypersaline conditions (55 PSU) in the three-culture medium (F/2, F/4, and F/8) with 123, 129, and 135 mg·L^{-1}, respectively (Fig. 2) showing significant differences ($p < 0.05$). Therefore, nitrogen concentration did not play an important role in biomass yield, unlike salinity. The chemical composition is directly affected by the combination of these factors (Table 1). In the most N-limited media, protein concentration decreases, especially in the F/4 and F/8 media. Carbohydrates increased at the F/2 and F/4 media at high salinity concentration (45 and 55 PSU), while at N-limited level (F/8) only at low salinities (25 PSU). The lipid concentration was affected only in the highest salinity (55 PSU) at the F/2 and F/4 media, decreasing its content, while in the other treatments it remained in similar concentrations. Salinity at 45 PSU in F/4 medium showed a decrease of ash (28.90 ± 1.64%), but an increase (49.90 ± 5.20%) at 55 PSU. Protein (28.90 ± 1.75%) was significantly high ($p < 0.05$) in the medium F/2 at salinities at 25 PSU. The highest concentration of lipids (30.45 ± 0.83%) was detected in the medium F/4 at 45 PSU. The amounts of lipids varied, and a significant ($p < 0.05$) reduction in this metabolite concentration was observed at 55 PSU. The highest value for carbohydrates (25.81 ± 2.66%) was observed in the medium F/2 at 55 PSU.

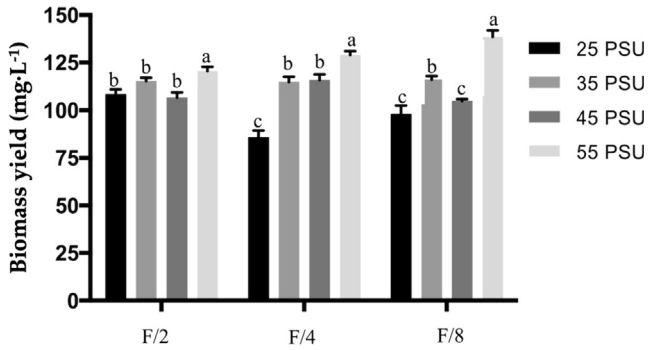

Fig. 2. Biomass yield (mg·L^{-1} of culture medium) of different culture conditions. The microalga was harvest at the end of the exponential phase. A different letter for each medium represents a significant difference ($P < 0.05$, one-way ANOVA per medium). Error bars correspond to standard deviation of triplicate cultures (n ≥ 3).

3.3. Central composite design and response surface methodology

Central Composite Design (CCD) matrix to statistical optimization of pigment production was calculated using JMP statistic software shown in Table 2. The experimental model used resulted in a second-order polynomial equation for each variable, representing the production of pigments as an effect of a combination of different factors for optimization of culture conditions. Besides, it is showing the support of the statistical model as a validation model. The effect of the four factors on the dependent variables is shown below.

3.4. Statistical optimization and response surface methodology on the chlorophyll a production

The validation model, presented as the second-order equation coefficients for prediction models for Chl *a* production, analysis of variance (ANOVA), lack of fit, and parameters estimate values, is shown in Table 3. Herein, the relationship is presented, and the effect among the processing factors and the culture condition for pigment production. ANOVA was performed to validate the equations of the quadratic models used for Chl *a* production. The analysis of parameter estimates showed that the four variables studied were the processing variables that most affected the Chl *a* production in linear terms ($P < 0.0001$). As for quadratic terms, only (day)^2 was significant ($P < 0.0001$), as evidenced by their low *p*-value. The interaction factors (Medium*Salinity), (Medium*-day), (Medium*Solvent) are significant ($P < 0.0001$) to evaluate the concentration of Chl *a*.

The model shows a not significant "lack of fit" ($p > 0.05$) that indicates no lack of adjustment in the model, which is favorable in the study. In a report made by Dahmoune et al. (2014), they observed that the small *p*-value in ANOVA ($P < 0.001$) indicates that the model can be used to optimize the growth condition variables, as shown in our study. The model fitting and second-order polynomial equations of Chl *a* in terms of coded factors is presented in Equation (6):

$$\begin{aligned} \text{Chl}a = {} & 0.6762 + (-0.0586)_{x1} + 0.0263_{x2} + 0.1426_{x3} \\ & + 0.0139_{x4} + 0.0076_{x1x2} + (-0.0585)_{x1x3} \\ & + (-0.0456)_{x1x3} + 0.032_{x2x3} + (-0.0036)_{x2x4} \\ & + (-0.017)_{x3x4} \\ & + 0.0084_{x1^2} + (-0.0766)_{x2^2} + 0.0122_{x3^2} + (-0.0036)_{x4^2} \\ & + error \end{aligned} \quad (6)$$

Table 1
Effect of different N-limited media and salinity level on chemical composition of *N. incerta*.

Media	Salinity (PSU)	Ash (%)	Protein (%)	Lipids (%)	Carbohydrates (%)
F/2	25	34.9 ± 3.3 ^{d,e}	28.9 ± 1.7 ^{a}	26.3 ± 0.8^{b}	9.7 ± 1.9 ^{d}
	35	49.6 ± 0.6 ^{a}	19.8 ± 0.4 ^{d}	25.5 ± 0.1^{b}	5.0 ± 0.8 ^{e}
	45	34.6 ± 0.6^{c,d}	22.3 ± 0.4^{c}	21.8 ± 1.6^{c}	21.3 ± 1.2^{b}
	55	33.1 ± 1.3 ^{d}	24.7 ± 1.9^{b,c}	16.3 ± 1.6 ^{d}	25.81 ± 2.6 ^{a}
F/4	25	39.6 ± 1.7^{b,c,d}	25.8 ± 0.4^{b,c}	24.6 ± 0.3^{b}	9.8 ± 0.8 ^{d}
	35	49.9 ± 0.8 ^{a}	16.8 ± 0.9 ^{ef}	25.1 ± 0.3^{b}	8.0 ± 0.3^{b}
	45	28.9 ± 1.6 ^{e}	26.7 ± 1.3 ^{a,b}	30.4 ± 0.8 ^{a}	13.9 ± 1.9 ^{d}
	55	49.9 ± 5.2 ^{a}	22.3 ± 0.4^{c}	15.4 ± 0.1 ^{d}	12.3 ± 1.9 ^{d}
F/8	25	38.7 ± 1.4^{b,c,d}	20.8 ± 1.0^{c,d}	20.4 ± 0.1^{c}	20.0 ± 0.9 ^{bc}
	35	44.5 ± 1.0 ^{a,b}	12.5 ^{g} ± 0.4 ^{g}	26.3 ± 0.1^{b}	16.6 ± 1.0^{c}
	45	45.4 ± 3.1 ^{a,b}	14.8 ± 1.7^{f}	22.3 ± 0.2^{c}	17.3 ± 1.7^{c}
	55	42.7 ± 1.4 ^{a,b,c}	16.6 ± 0.1^{c}	22.2 ± 0.1^{c}	18.3 ± 1.6^{c}

Values are mean ± standard deviation of at least three repetitions (n ≥ 3). Means followed by different lowercase letter in a same column are different at a significance level of 0.05. PSU = Practical Salinities Unity (g/kg).

Table 2
Central Composite design (CCD) matrix. Optimization of pigment production from microalgae *N. incerta*.

		Experimental variables				Responses		Predicted Responses	
Run	Pattern	X_1 (Medium)	X_2 (Salinity)	X_3 (Day)	X_4 (Solvent)	Chl *a* μg·mL^{-1}	T-Car μg·mL^{-1}	Chl *a* μg·mL^{-1}	T-Car μg·mL^{-1}
1	++−+	3	55	1	3	0.381	0.114	0.458	0.168
2	00a0	2	40	1	2	0.458	0.139	0.546	0.205
3	+++−	3	55	6	1	0.734	0.232	0.760	0.218
4	−−−−	1	25	1	1	0.391	0.098	0.407	0.125
5	000A	2	40	3.5	3	0.631	0.225	0.686	0.208
6	+−−−	3	25	1	1	0.559	0.054	0.483	0.018
7	0a00	2	25	3.5	2	0.444	0.144	0.573	0.201
8	+−−+	3	25	1	3	0.507	0.154	0.461	0.102
9	A000	3	40	3.5	2	0.631	0.229	0.626	0.246
10	a000	1	40	3.5	2	0.737	0.266	0.743	0.242
11	00A0	2	40	3.5	2	0.918	0.347	0.831	0.275
12	−−−+	1	25	1	3	0.570	0.156	0.567	0.153
13	−+−+	1	55	1	3	0.633	0.191	0.534	0.166
14	−−+−	1	25	6	1	0.832	0.279	0.779	0.209
15	000a	2	40	6	1	0.713	0.180	0.658	0.191
16	−++−	1	55	6	1	0.866	0.088	0.888	0.158
17	+−+−	3	25	6	1	0.546	0.173	0.621	0.216
18	++++	3	55	6	3	0.696	0.233	0.655	0.224
19	0A00	2	55	3.5	2	0.754	0.271	0.626	0.208
20	+−++	3	25	6	3	0.546	0.173	0.531	0.179
21	−+−−	1	55	1	1	0.349	0.118	0.388	0.095
22	++−−	3	55	1	1	0.490	0.050	0.494	0.041
23	−+++	1	55	6	3	0.866	0.088	0.965	0.107
24	0000	2	40	3.5	2	0.678	0.240	0.676	0.248
25	0000	2	40	3.5	2	0.678	0.240	0.676	0.249
26	−−++	1	25	6	3	0.900	0.089	0.872	0.116
27	*Control	1	35	3.5	2	0.687	0.243	0.253	0.217
28	**OT	2	40	3.5	2	0.891	0.369	0.856	0.321

Chl *a* = Chlorophyll *a*. T-Car = Total carotenoids.
Media: (1) F/2 = 0.88 mol·L^{-1}, (2) F/4 = 0.44 mol·L^{-1}, (3) F/8 = 0.22 mol·L^{-1} of nitrogen concentration. Salinity = PSU (Practical salinity Unity [g/kg]). Solvent: (1) Acetone, (2) methanol, (3) ethanol. g
* Control: 0.88 mol·L^{-1} of nitrogen; 35 PSU, measured at the end of the exponential phase and extracted with methanol.
** OT (Optimized treatment): 0.44 mol·L^{-1} of nitrogen; 40 PSU, 3.5 and extracted with methanol.

Table 3
Coefficients of the second order equations, prediction models for chlorophyll *a* production.

Analysis of variance					
Source of variation	DF	Sum of squares	Mean Square	F-Value	*P*-Value
Model	14	0.58	0.04	4.447	
Error	11	0.10	0.01	Prob > F	*P < 0.001*
C. Total	25	0.68		0.0087	
Lack of Fit					
Lack-of-Fit	10	0.10	0.10	Prob > F	*P > 0.10*
Pure Error	1	0.00	0.00		
Total Error	11	0.10			
Parameter estimates					
Source	DF	Coefficient	Standard error	F-Value	*P*-Value
Interceptor	1	0.680	0.038	18.96	< 0.0001*
X_1 (Medium: 1,3)	1	−0.059	0.022	15.83	< 0.0001*
X_2 (salinity: 25,55)	1	0.026	0.022	62.89	< 0.0001*
X_3 (Day: 1,6)	1	0.140	0.022	673.3	< 0.0001*
X_4 (Solvent: 1,3)	1	0.013	0.022	1.22	0.2939
X_1^2 (Medium*Medium)	1	0.008	0.060	0.14	0.5546
X_2^2 (salinity*salinity)	1	−0.077	0.060	0.08	0.7753
X_3^2 (Day*Day)	1	0.012	0.060	40.04	< 0.0001*
X_3^2 (Solvent*Solvent)	1	−0.004	0.060	0.06	0.1213
X_1 X_2 (Medium*Salinity)	1	0.008	0.024	38.59	< 0.0001*
X_1 X_3 (Medium*Day)	1	−0.059	0.024	51–16	< 0.0001*
X_1 X_4 (Medium*Solvent)	1	−0.046	0.024	−1.89	< 0.0001*
X_2 X_3 (Salinity*Day)	1	0.032	0.024	1.33	0.0003**
X_2 X_4 (Salinity*Solvent)	1	−0.004	0.024	42.04	< 0.0001*
X_3 X_4 (Day*Solvent)	1	−0.017	0.024	7.04	0.0010**

Fig. 3 shows the three-dimensional plot of the response variables obtained to model the curvature of the different responses directly affected by the independent variables. The maximum values are presented during logarithmic phases for all treatments, and all the studies showed a maximum point of around 40 PSU. Chlorophyll *a* showed the highest production, where the interaction between day-medium was significant (Fig. 3C), unlike the other interactions. Fig. 3A, B, and C show the maximum point outside the study area on the surface. That indicates that the study range was not satisfactory in the limits used to reach its optimum point. Besides, medium, salinity, and age of culture (day of harvest) were affected by the production of Chl *a*. The control surface plot

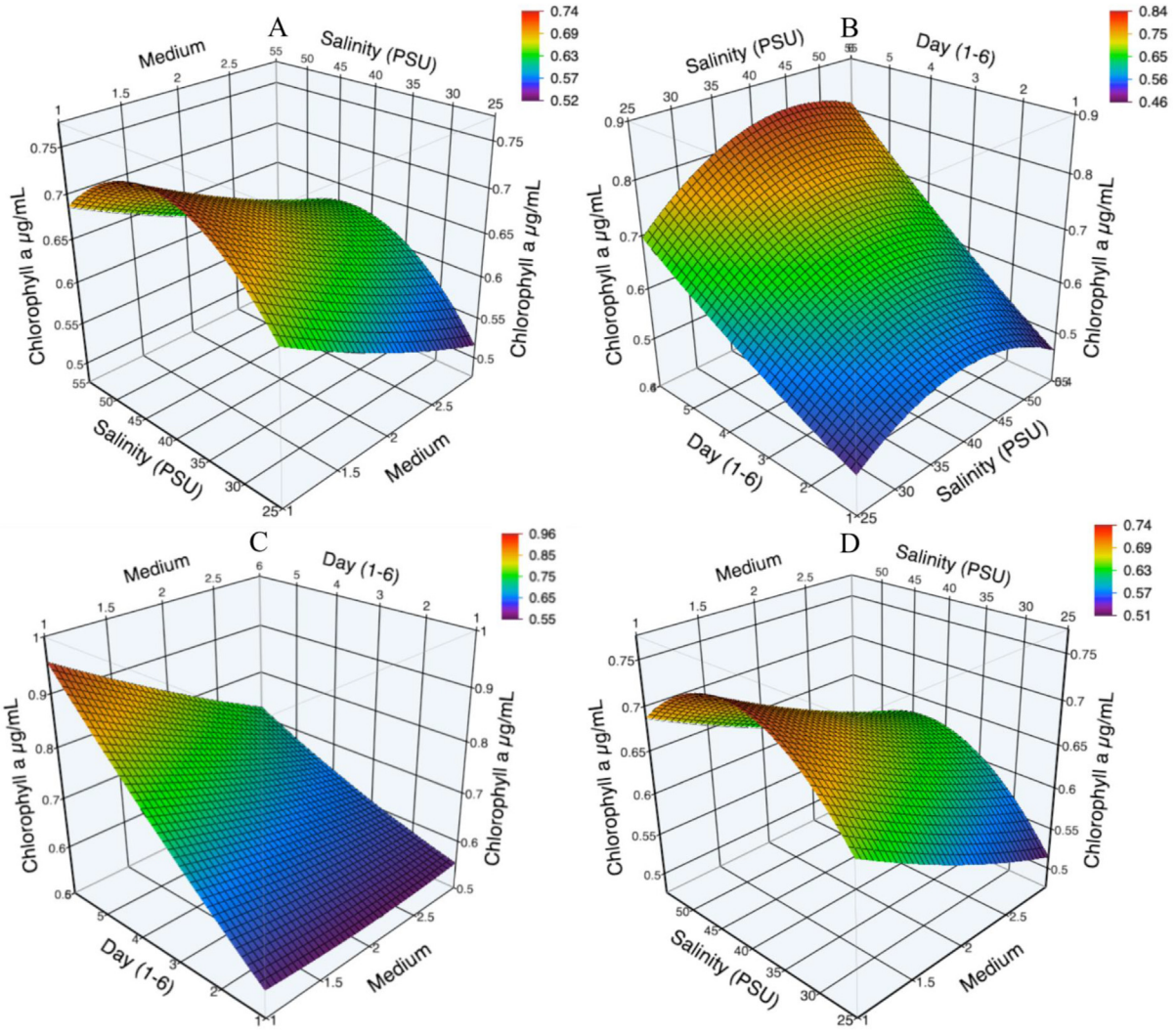

Fig. 3. Effects of the processing factors on chlorophyll *a* production: (A) Salinity ∗ Medium; (B) Day ∗ Salinity; (C) Day ∗ Medium and (D) Salinity ∗ Medium (control treatment).

(Fig. 3D) were similar to Fig. 3A. both were affected by the medium-salinity factor, showing approximate values (0.74 µg of Chl *a*·mL^{-1}). Fig. 3B (0.84 µg of Chl *a*·mL^{-1}) and C (0.96 µg of Chl *a*·mL^{-1}) exceeding the values shown by the control (0.74 µg of Chl *a*·mL^{-1}). The effect of the salinity-medium (Fig. 3A) and day-salinity (Fig. 3B) factors on the results of the chlorophyll concentration, including the control treatment (salinity-medium, Fig. 3D), showed the point maximum at a salinity of 40 PSU.

According to the results presented in Table 2, the treatment at F/8 medium, 55 PSU, the first day of age of culture extracted with ethanol shows the least producing Chl *a* (0.381 µg·mL^{-1}). The main factor that affected Chl *a* was the age of culture. On the first day, the microalga cells are found in the adaptation phase.

3.5. Statistical optimization and response surface methodology on the total carotenoids production

Table 4 presents the ANOVA, lack of fit, and parameter estimates by the second-order equation coefficients to prediction models for total carotenoid production. ANOVA shows the effects of the processing factor that had the most significant effect: salinity ($P < 0.0001$), day ($P < 0.0001$), solvent ($P < 0.0001$) and medium ($P < 0.0006$). The model for T-Car production shows a not significant "lack of fit" ($p > 0.05$) that indicates no lack of adjustment in the model. The model fitting and second-order polynomial equations of T-Car in terms of coded factors is presented in Equation (7):

$$\begin{aligned} \text{T}-\text{Car} = {} & 0.249 + 0.0022_{x1} + 0.0036_{x2} + 0.0349_{x3} + 0.0084_{x4} \\ & + 0.0133_{x1x2} + 0.0286_{x1x3} + 0.014_{x1x3} \\ & + (-0.0053)_{x2x3} + 0.0106_{x2x4} + (-0.0303)_{x3x4} \\ & + 0.0039_{x1^2} + 0.0439_{x2^2} + 0.0083_{x3^2} + (-0.0489)_{x4^2} \\ & + error \end{aligned} \tag{7}$$

The values obtained from this model are between 0.05 and 0.369 µg·mL^{-1} (Table 2). The maximum concentration of T-Car is presented during logarithmic phases. The values obtained in this model have a maximum point at 40 PSU. The factor that had the most significant effect was salinity ($P < 0.0001$). On the other hand, the interaction between solvent and salinity presented the optimum point on the response surface (Fig. 4B). Fig. 4 A, C, and D (control) show the maximum location inside the study area on the surface. That indicates that the study range was satisfactory. *i.e.*, the maximum points of the surface of each interaction were optimized. The significant interactions between day-salinity and

Table 4
Coefficients of the second order equations, prediction models for total carotenoids production.

Analysis of variance					
Source of variation	DF	Sum of squares	Mean Square	F-Value	*P*-Value
Model	14	0.11	0.07	2.105	
Error	11	0.04	0.03	Prob > F	*P < 0.001*
C. Total	25	0.15		0.1102	
Lack of Fit					
Lack-of-Fit	10	0.04	0.04	Prob > F	*P > 0.10*
Pure Error	1	0.00	0.00		
Total Error	11	0.04			
Parameter Estimates					
Source	DF	Coefficient	Standard error	F-Value	*P*-Value
Interceptor	1	0.248	0.024	6.78	< 0.0001*
X_1 (Medium: 1,3)	1	−0.002	0.014	7.51	0.0006**
X_2 (salinity: 25,55)	1	0.003	0.014	26.85	< 0.0001*
X_3 (Day: 1,6)	1	0.034	0.014	457.75	< 0.0001*
X_4 (Solvent: 1,3)	1	0.008	0.014	46.01	< 0.0001*
X_1^2 (Medium*Medium)	1	−0.004	0.038	3.63	0.0003**
X_2^2 (salinity*salinity)	1	−0.044	0.038	24.22	< 0.0001*
X_3^2 (Day*Day)	1	−0.008	0.038	5.1	0.0234***
X_3^2 (Solvent*Solvent)	1	−0.049	0.038	−1.30	0.0320***
X_1 X_2 (Medium*Salinity)	1	0.013	0.015	17.46	< 0.0001*
X_1 X_3 (Medium*Day)	1	0.029	0.015	43.92	< 0.0001*
X_1 X_4 (Medium*Solvent)	1	0.014	0.015	41.96	< 0.0001*
X_2 X_3 (Salinity*Day)	1	−0.005	0.015	4.08	0.0436***
X_2 X_4 (Salinity*Solvent)	1	0.016	0.015	5.25	0.0055**
X_3 X_4 (Day*Solvent)	1	−0.032	0.015	15.99	< 0.0001*

solvent-salinity affected the production of T-Car. Fig. 4A shows an increase in 5.8 days, and the optimal point would be found. Fig. 4 B presented a rise in six days, but it could be increased more if the culture is maintained for more days (12–14) to find the optimal point. All experimental treatments were superior to the control. The control surface plot (Fig. 4 D) was similar to Fig. 4 C, both were affected by the solvent-salinity factor, showing values of 0.74 μg of T-Car ·mL^{-1} and 0.24 μg of T-Car·mL^{-1}, respectively. The treatment at F/8 medium, 55 PSU, the first day of age of culture and extracted with ethanol, shows the minor producing T-Car (0.050 μg·mL^{-1}). The unfavorable culture conditions for carotenoids were the same as for Chl *a*. However, there was a decrease in the T-Car concentration of 83.5% between the best culture and the lowest concentration.

3.6. Model validation by the coefficients of determination

The main influence in the model was the salinity-solvent and salinity-medium interaction by total carotenoid. The salinity-medium (X_2 X_1) and salinity-solvent (X_2 X_4) interactions were significant ($p < 0.001$) for each variable response, whose interaction between these factors was used to obtain the best factor method to produce pigments. Predicted values were correlated with experimental to find the validity of the models for each response variables (Fig. 5). The coefficients of determination were r^2 = 0. 98 and r^2 = 0.92 (Chl *a*, and T-Car) indicating a high degree of dependence between the experimental values results and predicted by the equations. Based on the CCD and RSM results, the optimized treatment chosen was medium F/4, 40 PSU of salinity, at 3.5 days of age, and methanol solvent for extraction.

3.7. Antioxidant capacity assay

Methanolic, acetonic, and ethanolic extracts were made to evaluate the antioxidant activity. All extracts are potent reducing agents and exhibited antioxidant activity (Table 5 and 6). FRAP is an assay that uses a ferric salt in an oxidized state (Fe^{+3}) and by the action of an antioxidant (AOX) is reduced to Fe^{+2}. FRAP detects AOX with the ability of the SET (single electron transfer) mechanism but does not detect if the extracts are capable of inhibiting free radicals. The increase in ferric reduction (Fe^{+3} → Fe^{+2}) was observed in a time of 10 to 40 min (Table 5) for acetonic (672.90–766.03 μmol TE/g), methanolic (573.91–630.46 μmol TE/g), and ethanolic (390.16–483.29 μmol TE/g) extracts. The highest value (766.03 ± 16.62 μmol TE/g) was observed at 40 min in the acetonic extract. For the DPPH assay, all crude extracts showed no significant differences ($P > 0.05$) and low free-radicals capacity (33–35%) (Table 6). For that reason, it was not possible to determine the IC_{50} at the concentration of the extracts studied because the potency of the antioxidant in the extracts does not inhibit at least 50% of the $DPPH^{\bullet}$ radical, which makes it an essential characteristic to know the correct concentration. To determine the minimum inhibitory concentration (IC_{50}) is necessary to carry out radical inhibition kinetics at different antioxidant extract concentrations. Then, linear regression is used to accurately determine the concentration required to inhibit 50% of the radical. For the $ABTS^{\bullet+}$ radical, there were significant differences ($P < 0.05$) between the antioxidant activities of the extracts (Table 6). The acetonic and methanolic extracts presented the highest inhibition percentage (92.16 ± 0.16 and 91.50 ± 0.01%, respectively). The IC_{50} were 202.47 ± 8.54 μg of pigment·mL^{-1} in acetonic and 232.61 ± 6.67 μg of pigment ·mL^{-1} in methanolic extracts. The AAPH· radical showed a significant difference between the three extracts (Table 6). The methanolic extract presented the highest and great free radical-scavenging capacity (96.72 ± 0.01%) with an IC_{50} of 21.43 ± 1.16 μg of pigment·mL^{-1}. From the opposite view, the ethanolic extract showed the lowest inhibition activity among the extracts with 86.27% of inhibition and IC_{50} 251.83 ± 12.18 μg of pigment mL^{-1} with $ABTS^{\bullet+}$, and with AAPH presented 81.86% of inhibition and IC_{50} 535.85 ± 13.33 μg of pigment mL^{-1}.

3.8. Protective activity on oxidative damage in human erythrocytes

Fig. 6 shows the characteristics and morphological changes of the erythrocyte damage induced by the radical AAPH and the protection of *N. incerta*. The radical AAPH induces oxidation of lipid membrane and proteins and eventually causes erythrocytes hemolysis (Tai et al., 2011). The radical can be inhibited by the

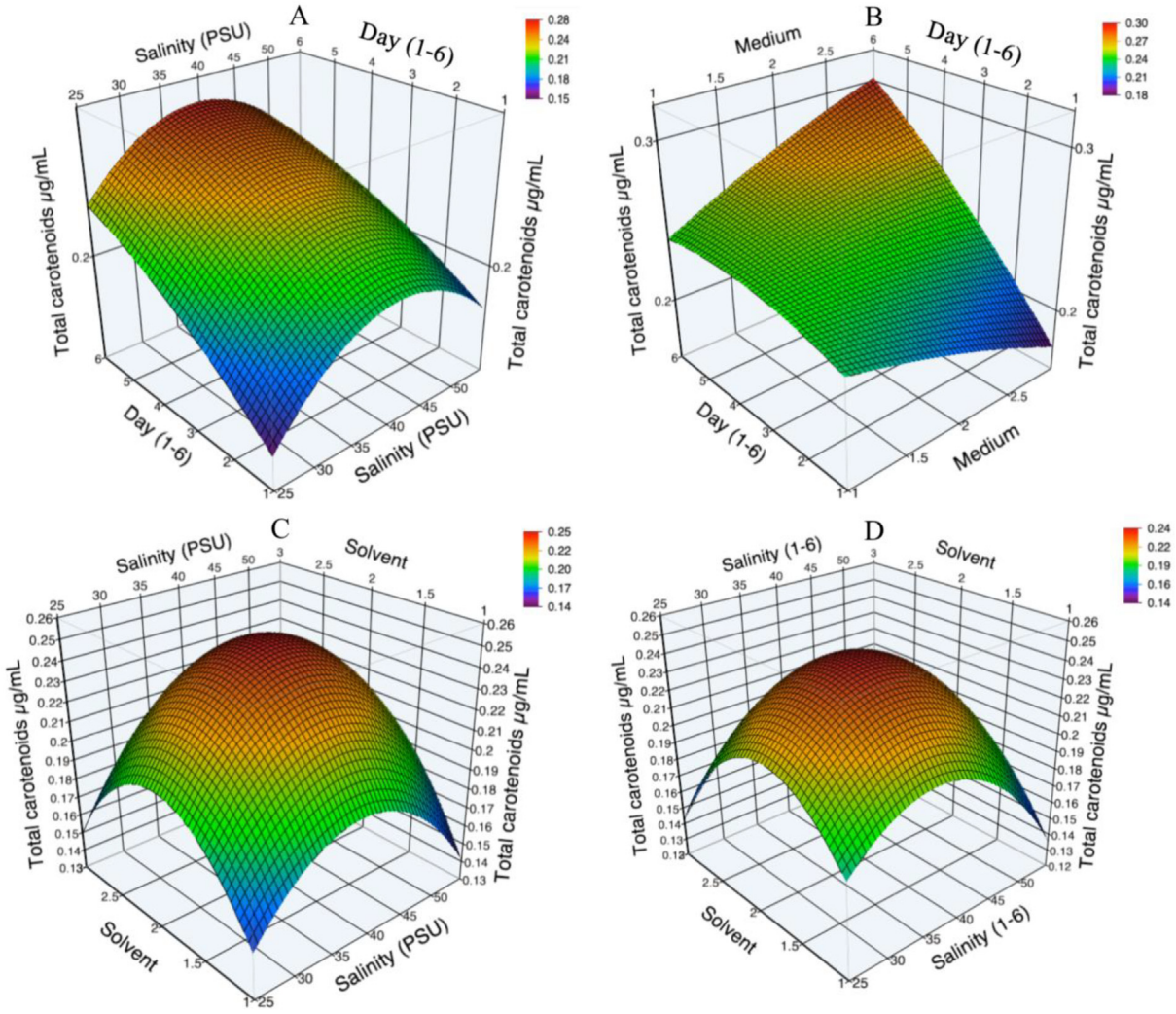

Fig. 4. Effects of the processing factors on total carotenoids production of *N. incerta*: (A) Day ∗ Salinity; (B) Day ∗ Medium; (C) Solvent ∗ Salinity and (D) Solvent ∗ Salinity (control treatment).

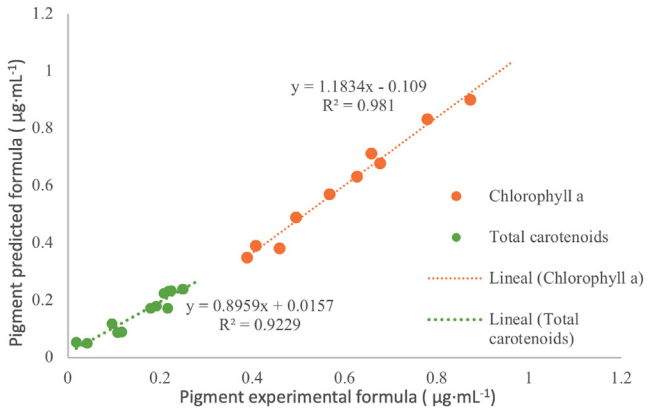

Fig. 5. Experimental vs.predicted value for pigment production by an extract from *N. incerta.*

antioxidants found in the extracts of the microalga *N. incerta*, avoiding hemolysis and morphological changes in erythrocytes. A suspension of erythrocyte (Fig. 6 A) and AAPH with erythrocytes (Fig. 6 B) controls were used to identify the severity of the radical on the red cells. Additionally, hemolysis caused by the radical AAPH (Fig. 6 B) was compared with hemolysis caused by autoimmune hemolytic anemia (Fig. 6 C). It can be observed that the hemolysis caused by the radical AAPH was destructive in comparison to the control of erythrocyte suspension. A high protective effect against the radical AAPH was found. The components of the extracts (acetonic, methanolic, and ethanolic) were able to inhibit cell damage (Fig. 6 D, E, and F). The treatments show typical red blood cells have an oval, biconcave, flattened shape, with a depression in the center and diameter of a normal erythrocyte of 6–8 µm (Fig. 6 D, E, and F). The optimized extract had a high free radical-scavenging capacity and ferric reducing antioxidant power; besides, it avoided the cellular damage caused by the radical AAPH. The protection of healthy cells such as erythrocytes is a crucial feature since, in future studies, it can be investigated whether these extracts compounds can reduce the cancer cells viability without damaging healthy cells.

4. Discussion

Primary and secondary metabolites of microalgae are directly affected by nutrient and saline stress conditions. One factor contributing to a higher biomass yield was obtaining a higher cell density in the cultures at high salinities (55 PSU). The osmoregulation process in microalgae intervenes in hypersaline conditions, result-

Table 5
Ferric reducing antioxidant power of extracts obtained from *N. incerta.*

Extracts	µmol TE/g dry biomass ± SD FRAP value at different times (min)			
	10	20	30	40
Acetonic	672.9 ± 18.2 ^{aB}	685.9 ± 16.6 ^{aB}	678.5 ± 28.2 ^{aB}	766.0 ± 16.6 ^{aA}
Methanolic	573.9 ± 23.3 ^{bB}	582.0 ± 13.1 ^{bAB}	608.5 ± 21.3 ^{bAB}	630.4 ± 23.3 ^{bA}
Ethanolic	390.1 ± 6.7 ^{cC}	427.2 ± 15.5 ^{cB}	479.9 ± 15.8^{cA}	483.2 ± 6.7 ^{cA}

[1]Values are mean ± standard deviation (SD) of three repetitions. One-way ANOVA, with post hoc analysis (Tukey test), is indicated by a different letter for each response variable (per extract and reaction time). Means followed by a different lowercase letter in the same column indicate significant differences ($p < 0.05$) between the extracts tested. Values followed by a different uppercase letter in the same row indicate significant differences ($p < 0.05$) between the reaction time tested for each extract.

Table 6
Percentage of inhibition of DPPH, ABTS and AAPH assays exposed of the different extracts of pigments from *N. incerta* by effect of free radical-scavenging capacity assay.

Extract	% of inhibition			IC_{50} (µg/mL)		
	DPPH	ABTS	AAPH	DPPH	ABTS	AAPH
Acetonic	35.3 ± 0.3 ^{a}	92.1 ± 0.1 ^{a}	89.2 ± 0.7^{b}	>780	202.4 ± 8.5 ^{a}	101.7 ± 8.1^{b}
Methanolic	35.2 ± 0.2 ^{a}	91.0 ± 0.2 ^{a}	96.7 ± 1.1 ^{a}	>780	232.6 ± 6.6^{b}	21.4 ± 1.1 ^{a}
Ethanolic	33.4 ± 0.4 ^{a}	86.2 ± 0.1^{b}	81.8 ± 3.2^{c}	>780	251.83 ± 12.1^{b}	535.8 ± 13.3^{c}

The concentration of the extracts was 780 µg·mL^{-1}
IC_{50} Minimum inhibitory concentration to inhibit at least 50% or the radical ($n \geq 3$).
[1]Values are mean ± standard deviation of at least three repetitions. Means followed by different lowercase letter in a same column are different at a significance level of 0.05.

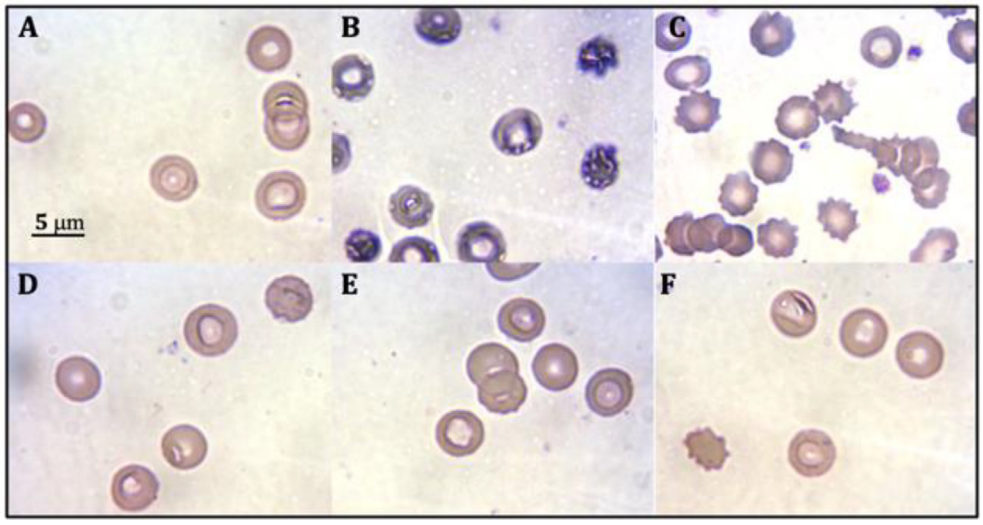

Fig. 6. Protective activity on oxidative damage in human erythrocytes. Micrographs of human erythrocytes (100x). Induction of hemolysis with the radical AAPH. (A) Control (-): erythrocytes without radical. (B) Control (+): erythrocytes with radical (hemolysis). (C) Reference control: autoimmune hemolytic anemia. (D) Acetone extract with radical (E) Methanolic extract with radical (F) Ethanolic extract with radical.

ing in a considerable increase in cell density. That has been observed in different microalgae species, such as marine diatom pseudo-*Nitzschia* (Ayache et al. 2020). There is an accumulation of primary compounds such as proteins, lipids, and carbohydrates, and minerals used as mediators in biochemical cycles of cellular stress regulation (Gonçalves et al., 2019). An increase in biomass might be caused by an increase in its primary metabolites, such as lipids (Table 2) that might confer better resistance to the plasma membrane damaged by the intense salinity (Benavente-Valdés et al., 2016)**.** It has been reported that for microalgae chlorophytes, the decrease in the nitrogen content in the medium has an unfavorable impact on the biomass yield, presenting a considerable reduction (Goiris et al., 2015). Our results show that the variables salinity and low-nitrogen concentrations were more significant factors for the growth of the microalga *N. incerta*. The maximum cell concentration (688,750 ± 29,509 cell·mL^{-1}) was shown in the most N-limited medium (F/8 = 0.22 mol·L^{-1}N) in hypersaline conditions (55 PSU). Suggesting that metabolic cycles are more affected by these variables resulting in a higher cellular concentration. The difference in these results may be due to the species used and the experimenťs design. Fimbres-Olivarría et al. (2010) studied the growth of *Navicula* sp. cultured using a nitrogen concentration of 0.88 mol·L^{-1} (F/2 medium) at a salinity of 35 PSU. They obtained a maximum cell density of 291,875 cell·mL^{-1}. While in our study with the same conditions obtained approximately 480, 000 cell·mL^{-1}.

Not only replication is affected by different environmental variables, but also the chemical composition of the microalgal biomass based on stressed media. Light intensity, wavelength, salinity, and nitrogen source are the most critical factors contributing to biomass composition. Few studies on genus *Navicula* involve the combined effect of these variables on the chemical composition. Several microalgae species like *Isochrysis aff. galbana* (clone T-ISO) and *Nannochloropsis oceanica* decreased with increased N-limitation (45 and 37%, P < 0.05); meanwhile, *Rhodomona. baltica* and *Pheodactilum tricornotum* showed no change in their chemical

composition under N limitation (Wang et al., 2019). However, in our study, the concentration of protein and carbohydrates were directly affected by nitrogen deficiency, while the lipids were altered by salinity. Therefore, it carries out an osmoregulation process reflected in the lipids production; but the effect of nitrogen deficiency on the medium is not ruled out. Additional to the variable's salinity and nitrogen concentration, light intensity and irradiance are essential factors to consider. These are not only factors considered in photosynthesis and pigment production, also directly affect the content of microalgae metabolites. The light intensity and wavelength have been observed to be critical factors. In the study by Fimbres-Olivarría et al. (2015), it was seen that under blue light at a light intensity of 50 μmol photon/m^2/sec, the highest protein (22.83 ± 2.42%) and lipid (25.32 ± 5.32%) concentration was presented. However, our study revealed not so much difference in the protein (26.70 ± 1.3%) and lipid (30.40 ± 1. 3%) contents, with white wavelength (400–750 nm) an intensity of 100 μmol photon/m^2/sec. Hence, in comparison with the reference and our results, we observed that the factors salinity and nitrogen concentration are more significant for producing these macromolecules in the genus *Navicula*.

Numerous studies have shown the impact of nutrients on the accumulation of lipids and the decrease of proteins due to nitrogen limitation (Wang et al., 2019). This similar behavior was observed in our results. However, the accumulation of lipids, carbohydrates, and ash were influenced to a greater extent by salinity conditions (Table 1). The increase of the mineral fraction could be related to osmotic pressure triggering silicateś production as a protector effect by the osmoregulation cell. The protein showed a decrease in the most limited medium in nitrogen, only at normal and high salinity conditions (35, 45, and 55 PSU). Photosynthesis mainly requires chlorophylls. The base structure comprises four nitrogen atoms attached to a metal core (Mg^{2+}) in its porphyrin ring. Therefore, under the conditions mentioned above, the adaptive efficiency of *N. incerta* required a higher load of chlorophylls to maintain its survival. Table 2 shows the variation of chlorophylls in different treatments. It is worth noting not only chlorophyll *a* can increase or decrease, but also total chlorophylls. Additionally, it should be taken into account that during growth and adaptation nitrogen-limited concentrations, enzymes that require nitrogen can be found (Brown et al., 1996; Calderon et al., 2016) and could be involved in the synthesis of lipids (or other metabolites), since in the medium F/8 at 55 PSU an increase in this metabolite is observed, unlike F/2 and F/4 media at this same salinity (55 PSU).

The high salinities and low-nitrogen concentration as a stress factor influenced carotenoids accumulation. These factors generate carotenoids synthesis and should be considered in developing products based on microalgae (Markou and Nerantzis, 2013). Carotenoids are essential for microalgae as accessories pigments, but as that they act as a protective barrier against high light radiations dissipating excess energy (Hu et al., 2018; Barajas-Solano et al., 2020). Therefore, nitrogen is one of the critical nutrients in the microalgae metabolic cycles (Beardall et al., 2001). When the microalgae are limited in nitrogen (N), but the other components are kept in their correct proportions, photosynthesis can continue. Nitrogen-rich components decrease (as protein), but carotenoids increase. Nitrogen-depleted cells can transform non-lipid to lipids and carotenoids compounds (Richmond, 2004). In this way, there are increases in non-photochemically active carotenoid pigments. However, the decrease in protein synthesis affects photochemical energy distribution (Berges et al., 1996). Cells with low-nitrogen concentration use chlorophylls as a storage source for this mineral. In this way, nitrogen is easily infused and accessible for microalgae development (Li et al., 2008). For example, *Chlamydomonas reinhardtian* and *Scenedesmus subspicatus* depend on nitrogen levels to start their different development stages. In nitrogen limitation, they enter their stationary phase (Dean et al., 2010). Nitrogen sources have been observed to influence the development of the microalgae and its components directly, for example, ammonium nitrate has less impact on the production of biomass and carotenoids (Imamoglu et al., 2009). In our case, sodium nitrate was used to rapidly stimulate the microalgal physiological response under nitrogen-deficient conditions, triggering carotenoid biosynthesis. A similar condition was used by Touchette and Burkholder (2000). In general, low-nitrogen concentrations have a more significant impact than excess nitrogen for these pigments. Carotenoids such as lutein, β-carotene, astaxanthin, and canthaxanthin, begin to accumulate in the microalgae in response to nitrogen deficiency (Borowitzka et al., 1991; Del Campo et al., 2000; Abe et al., 2007).

The second most crucial factor for carotenoid synthesis is the concentration of salinity. That is due to effects on physiological processes and nitrogen deficiency, e.g., metabolite content (Kumar et al., 2010) and photosynthetic efficiency (Rijstenbil, 2005). Changes in the membrane characteristics are another effect of salinity in the culture medium (Kooijman et al., 2005). In these cases, carotenoids are used as protective barriers. Osmoregulation is essential for the intracellular stability and metabolic efficiency of microalgae. Under hypersaline conditions, bioactive compounds synthesis increases, and thus their accumulation, unlike hyposaline conditions (Yancey, 2005). This characteristic occurs in diatoms such as *N. incerta*, generating mechanisms of tolerance to salinity. However, these mechanisms have not been fully elucidated to carry out a more efficient understanding.

Factors as salinity and nitrogen deficiency were favorable for the production of antioxidant pigments. Optimization studies demonstrate significantly enhance pigment production to obtain maximum efficiency that could be implemented in various industrial sectors (Lefsih et al., 2017). The CCD is applied to experimental data that cannot be described by linear functions. The second-order equation application allowed the results to be evaluated as surfaces of quadratic responses, raising the independent variables squared. According to Fratoddi et al. (2018), the equations of each response variable depend on the ANOVA results. The initial results suggest that the high salinities and nitrogen-limited concentration increase the cellular concentration of the microalga. It has been found that *N. incerta* grows in high salinity around 12 to 14 days (Affan et al., 2007; Kyong-Hwa et al., 2011; Sánchez Saavedra and Núñez, 2012). There are no reports of its response to nitrogen-limited concentrations. In our study, the interaction between high salinities and nitrogen-limited concentrations resulted in a rapid replication rate (around 1 div·day^{-1}) with the maximum growth rate. However, benthonic microalga *N. Incerta* can be influenced by their growth, temperature, salinity, and nutrient concentration (Lewin and Lewin, 1960; Sánchez Saavedra and Núñez, 2012). On the other hand, nitrogen is used for DNA and protein synthesis, necessary for survival and reproduction. The microalgae limit the production of Chl *a* in quantities required for photosynthesis (Brown et al., 1996). That could explain the variation observed in Chl *a* in Table 2.

Response surface methodology was applied to modeling the effect of variables and interaction of different growth conditions to produce pigments of *N. incerta*. The variability depends on several factors during the growing conditions as the nutrients in the medium, age of culture, salinity and the solvent used for the extraction. The solvent had an important role in obtaining antioxidant pigments since each pigment is extracted in different quantities, due to polarity (Baudelet et al., 2013; Burboa-Zazueta et al., 2018). In our study, nitrogen deficiency and high salinities increased the chlorophylls and carotenoids content. Still, these results contradict those of Richmond (2004), Gong and Bassi (2016), Mustafa et al. (2019), and Wai Kuan (2019). Those authors observed a significant reduction in the production of these pig-

ments in *Dunaliella* sp. *Nitzquia* sp., *Scenedesmus* sp., *Phaeodactylum tricornutum, Tetraselmis suecica*, *Nanofrustulum shiloi*, and *Chlorella vulgaris*. These differences were due to the species used and the interaction between the high salinities and the design of advanced experiments (DOE) used in our research. With the use of DOE tools, the curvature modeling allows us to observe the variable responses directly affected by nitrogen limitation and salinity, increasing the antioxidant capacity. Undoubtedly, response surface methodology proved to be a very useful tool for obtaining a maximum of antioxidant pigments, and methanol as the solvent has shown great potential to extract chlorophylls and total carotenoids from *N. incerta.* The factors studied are considered the most important physical factors (Araujo and Garcia, 2005; Muller Feuga et al., 2007). In nature, climate change affects phytoplankton growth, giving complex biological effects since it is considered that salinity imposes the highest metabolic requirements for the synthesis of secondary metabolites such as chlorophylls and carotenoids (St. John et al., 2001).

The acetonic, methanolic, and ethanolic pigment extracts showed high ferric reducing antioxidant power (390–766 μmol TE/g dry biomass) measured by FRAP assay (Table 5). The FRAP assay depends on the compounds redox potential, where the reducing power of chlorophylls and carotenoids are associated with reducing double (-C = C-) and allenic (-C = C = C-) bonds that can donate electrons. It has been demonstrated that these bonds exert a significant antioxidant capacity. In the study of Hajimahmoodi et al. (2010), they found that several microalgae, including *Chlorella vulgaris* and *Nostoc muscorum*, had the highest antioxidant capacity (58.21 ± 16.62 and 63.26 ± 6.15 μmol TE/g dry biomass, respectively) by the FRAP assay. Besides, microalgae such as *Haematococcus pluvialis*, *Isochrysis* T-ISO, *Isochrysis* sp., *Phaedactylum tricornutum,* and *Tetraselmis* sp., showed values around of 46–89 μmol TE/g dry biomass (Gong and Bassi, 2016). In our study, the ferric reducing antioxidant power is higher than these references being the acetonic extract the highest (766.0 ± 16 .6 μmol TE/g dry biomass). The difference between the values of the previous studies and our study may be due to the optimization methodology used to obtain antioxidant pigments and the solvents used for their extraction.

Results also showed that the three pigment extracts (acetonic, methanolic, and ethanolic) have the a high free radical-scavenging capacity inhibiting 81–92% in $ABTS^{\bullet+}$ and 81–96% in AAPH (used as hemolytic agent). Lower inhibition (33–35%) in $DPPH^{\bullet}$ radical was observed by the pigment extracts (Table 6). The free radical-scavenging capacity of pigment extracts is attributed to chlorophylls, carotenes, and xanthophylls (Chuyen and Eun, 2017). Therefore, the double bond system forms the admission of radical species ($ROO^{\bullet}$ (radical) + AOX → ROO^{-} $AOX^{\bullet}$). The variations between the free radical-scavenging capacity can be attributed to the polarity solvent and radical inhibition mechanism, susceptible to electron donation (SET). For this reason, the desired potency was not enough to inhibit the $DPPH^{\bullet}$ radical because this radical presents a proton transfer or hydrogen removal (HAT) mechanisms. The pigments extract of *N. incerta* can be of high affinity for the $ABTS^{\bullet+}$ radical due to its lipophilic and hydrophilic radical, while the DPPH radical is a more selective radical (Prior et al., 2005).

The generation of free radicals induces increased carotenoid accumulation in several microalgae species such as *Dunaliella* sp, *Nitzquia* sp, and *Scenedesmus* sp at nitrogen-limited concentrations and hypersaline conditions, increasing their antioxidant activity (Gong and Bassi, 2016; Mustafa et al., 2019). Similar behavior was shown in our study. Micronutrients such as nitrogen, phosphorus, and silicon regulate the synthesis of chlorophylls and carotenoids with antioxidant power in diatom (Fu et al., 2015). On the other hand, several studies have shown the low capacity of microalgae extracts to inhibit the DPPH radical. Saranya et al. (2014) observed that the methanolic and acetonic extracts of *Isochrysis galbana*, *Chaetoceros calcitrans,* and *Chlorella salina* are around 14–34% inhibition of the $DPPH^{\bullet}$ radical, which are similar to our optimized extracts of *N. incerta*. However, the extracts of *Nostoc muscorum* showed a high inhibition of the $ABTS^{\bullet+}$ (81.6%), similar to our results. It should be noted that the concentration used in the extract of *Nostoc muscorum* that the inhibition test was higher (30 $mg{\cdot}mL^{-1}$) than that from our study (780 $\mu g{\cdot}mL^{-1}$). Recent studies have shown that organic solvents influence the obtention of antioxidant pigments from microalga because the % of inhibition performed in an aqueous extract is low for $ABTS^{\bullet+}$ and $DPPH^{\bullet}$ as is the case of the microalga *Rhodosorus marinus* that showed 5.59 ± 0.63% $ABTS^{\bullet+}$ inhibition and 25.60 ± 4.03% $DPPH^{\bullet}$ radical inhibition (Burboa-Zazueta et al., 2018). However, in our case, the three pigment extracts (methanolic, acetonic, and ethanolic) presented low DPPH inhibition, probably attributed to composition.

About the anti-hemolytic assay, the AAPH used is broken down into molecular nitrogen and carbon radicals that can combine to produce stable compounds or produce peroxyl radicals by reacting with molecular oxygen, causing lipid peroxidation. That affects living cells plasma membranes such as human erythrocytes that promote the formation of holes in the cell membrane, expelling its content, causing changes in the erythrocyte morphology (Liu and Finley, 2005). These morphological changes present in the positive control in our study correspond to the formation of exogenous vesicles that transport material outside the membrane, such as hemoglobin, enzymes, and different types of proteins, causes the cell death induced by AAPH (Finkel and Holbrook, 2000). According to our results made by optical microscopy (Fig. 6), the extracts probably create a biofilm formed by chlorophylls and carotenoids, since the optimized extract has a high amount of these metabolites. Erythrocyte micrographs revealed a slight greenish coloration, which could be formed by hydrophobic interactions pigment-erythrocyte plasma membrane. The pigments inhibit oxidation and the consequent cellular damage caused by free radicals, very reactive substances that introduce oxygen into the cells inducing alterations in the DNA and various changes that accelerate the aging of the body (Liu and Huang, 2015). That could explain the high anti-hemolytic activity (81–96%) by the pigment extracts.

5. Conclusion

In conclusion, our study defines the factors of salinity and nitrogen deficiency favorable for antioxidant pigments production. A substantial amount of chlorophyll *a* and total carotenoids of *N. incerta* was obtained with strong antioxidant capacity and anti-hemolytic activity. Optimization studies significantly enhanced pigment production to obtain maximum efficiency that could be implemented in various industrial sectors. The results demonstrated that response surface methodology was a useful tool to optimize the growth condition to obtain biomass in a short time and cost reduction. According to the overlay plots, the optimum growth condition to obtain Chl a and T-Car were medium = F/4 (0.44 $mol{\cdot}L^{-1}$), salinity (PSU) = 40, age of culture (day) = 3.5, and solvent = methanol. The antioxidant activity of *N. incerta* Chl *a* and T-Car indicated that they had a high ability to $ABTS^{\bullet+}$ and AAPH free radical-scavenging and carried out the oxide-reduction increase of the ferric reduction ($Fe^{+3} \rightarrow Fe^{+2}$). The optimized extraction shows a potential anti-hemolytic activity to avoid the morphological change of human erythrocytes. These results provide a basis for future research on the biological activity characterization and use as a chemopreventive agent of chronic non-communicable

diseases of high social impact and its application in developing functional foods or its use as a drug.

Author contribution

R. I. González-Vega and C.L Del-Toro-Sánchez developed the concept, designed the study, conducted the experiments, and interpreted the results. J.L. Cárdenas-López contributed to design the experiment and interpreted the results of statistical optimization. J. A. López-Elías contributed with the aquaculture laboratory and with the cultivation of the microalga. S. Ruiz Cruz contributed with the anti-hemolytic activity analysis. A. Reyes-Díaz and L. M and Pérez-Pérez. contributed with the antioxidant activity assays. F.J. Cinco-Moroyoqui helped in polishing the language and improving the manuscript. R. E. Robles-Zepeda helped with the sample preparation and the interpretation of micrographs of human erythrocytes. J. Borboa-Flores provided scientific guidance throughout the study and all sources of funding. All authors reviewed and approved the manuscript.

Declarations

Founding information

This research did not receive any specific grant from funding agencies in the public, commercial, or not-for-profit sectors.

Declaration of Competing Interest

The authors declared that there is no conflict of interest.

Acknowledgements

Author R.I. González-Vega acknowledges for the graduate scholarship granted from the Consejo Nacional de Ciencia y Tecnología (CONACyT, Mexico).

References

Abe, K., Hattori, H., Hirano, M., 2007. Accumulation and antioxidant activity of secondary carotenoids in the aerial microalga *Coelastrella striolata* var. multistriata. Food Chem. 100, 656–661. https://doi.org/10.1016/j.foodchem.2005.10.026.

Affan, A., Rohan, K., You-Jin, J., Joon-Baek, L., 2007. Growth characteristics and antioxidant properties of the benthic diatom *N. incerta* (Bacillariophyceae) from Jeju island. J. Phycol. 43, 823–832. https://doi.org/10.1111/j.1529-8817.2007.00367.x.

Agcam, E., Akyıldız, A., Balasubramaniam, V.M., 2017. Optimization of anthocyanins extraction from black carrot pomace with thermosonication. Food Chem. 237, 461–470. https://doi.org/10.1016/j.foodchem.2017.05.098.

Almeida, M., Erthal, R., Padua, E., Silveira, L., Am, L., 2008. Response surface methodology (RSM) as a tool for optimization in analytical chemistry. Talanta 76, 965–977. https://doi.org/10.1016/j.talanta.2008.05.019.

Altan, A., McCarthy, K.L., Maskan, M., 2008. Extrusion cooking of barley flour and process parameter optimization by using response surface methodology. J. Sci. Food Agricultur. 88, 1648–1659. https://doi.org/10.1002/jsfa.3262.

AOAC, 1997. Official methods of analysis. Assn. of Official Analytical Chemists, Gaithersburg, Md..

AOAC. 2000. Association of Official Analytical Chemists. Official methods of analysis of AOAC. 19th ed, 2012. Arlington.

USA.Araujo, S.C., Garcia, V.M.T., 2005. Growth and biochemical composition of the diatom Chaetoceros cf. wighamii brightwell under different temperature, salinity, and carbon dioxide levels. I. Protein, carbohydrates, and lipids. Aquaculture 246, 405-412. https://doi.org/10.1016/j.aquaculture.2005.02.051.

Athmouni, K., Belhaj, D., El Feki, A., Ayadi, H., 2017. Optimization, antioxidant properties and GC-MS analysis of Periploca angustifolia polysaccharides and chelation therapy on cadmium-induced toxicity in human HepG2 cells line and rat liver. Int. J. Biol. Macromol. 108, 853–862. https://doi.org/10.1016/j.ijbiomac.2017.10.175.

Ayache, N., Hervé, F., Lundholm, N., Amzil, A., Caruana, A.M., 2020. Acclimation of the marine diatom pseudo-Nitzschia australis to different salinity conditions: effect on growth, photosynthetic activity, and domoic acid content. J. Phycol. 56 (1), 97–109. https://doi.org/10.1111/jpy.12929.

Baudelet, P.H. et al., 2013. Antiproliferative Activity of *Cyanophora paradoxa* Pigments in Melanoma, Breast and Lung Cancer Cells. Marin Drugs. 11, 4390–4406. https://doi.org/10.3390/md11114390.

Barajas-Solano, A,F., Guarin-Villegas, E., Remolina-Páez, L.M., Bermúdez-Castro, J.P., Mogollón-Londoño, S.O., Contreras-Ropero, J.E., García-Martínez, J.B., 2020. Effect of de Carbon/Nitrogen ratio on the production of microalgae-based carotenoids. Ingeniería y Competitividad. 22(1), 8686. doi.org/10.25100/iyc.v22vi1i.8686.

Beardall, J., Young, E., Roberts, S., 2001. Approaches for determining phytoplankton nutrient limitation. Aquat. Sci. 63, 44–69. https://doi.org/10.1007/PL00001344.

Benavente-Valdés, J.R., Aguilar, C., Contreras-Esquivel, J.C., Méndez-Zavala, A., Montañez, J., 2016. Strategies to enhance the production of photosynthetic pigments and lipids in chlorophycae species. Biotechnol. Rep, 10, 117–125. https://doi.org/10.1016/j.btre.2016.04.001.

Benzie, I., Strain, J., 1996. The ferric reducing ability of plasma (FRAP) as a measure of "antioxidant power": The FRAP assay. Anal. Biochem. 239, 70–76. https://doi.org/10.1006/abio.1996.0292.

Berges, J.A., Charwbois, O.D., Mauzerall, D.C., Falkowski, P.G., 1996. Differential effects of nitrogen limitation on photosynthetic efficiency of photosystems I and II in microalgae. Plant Physiol. 110. https://doi.org/10.1104/pp.110.2.689.

Bezerra, M.A., Santelli, R.E., Oliveira, E.P., Villar, L.S., Escaleira, L.A., 2008. Response surface methodology (RSM) as a tool for optimization in analytical chemistry. Talanta 76, 965–977. https://doi.org/10.1016/j.talanta.2008.05.019.

Borowitzka, M.A., Huisman, J.M., Osborn, A., 1991. Culture of the astaxanthin-producing green alga *Haematococcus pluvialis*. Effects of nutrients on growth and cell type. J. Appl. Phycol. 3, 295–304 https://link.springer.com/content/pdf/10.1007/BF02392882.pdf.

Brown, R.M., Dunstan, A.G., Norwood, N.S., Miller, A.K., 1996. Effects of harvest stage and light on the biochemical composition of the diatom *Thalassiosira* pseudonana. J. Phycol. 32, 64–73. https://doi.org/10.1111/j.0022-3646.1996.00064.x.

Brand-Williams, W., Cuvelier, M., Berset, C., 1995. Use of a free radical method to evaluate antioxidant activity. LWT-Food Sci. Technol. 28, 25–30. https://doi.org/10.1016/S0023-6438(95)80008-5.

Burboa-Zazueta, M.G., Gutiérrez-Millán, L.E., Valdéz-Covarrubias, M.A., López-Torres, M.A., Burgos-Hernández, A., Garcia-Galaz, A., 2018. Actividades biológicas del extracto metanólico de *Rhodosorus marinus*. Biotecnia. XX (3), 102–110.

Calderon Oliver, M., Escalona Buendía, H., Medina Campos, O.N., Pedraza Chaverri, J., Pedroza Islas, R., Ponce Alquicira, E., 2016. Optimization of the antioxidant and antimicrobial response of the combined effect of nisin and avocado byproducts. LWT-Food Sci. Technol. 65, 46–52. https://doi.org/10.1016/j.lwt.2015.07.048.

Chih Wei, C., Ching Chi, Y., Ming Tsang, W., Mei Chich, H., Yu Tse, W., 2017. Microwave-Assisted Extraction of Cannabinoids in Hemp Nut Using Response Surface Methodology: Optimization and Comparative Study. Molecules 22, 1894. https://doi.org/10.3390/molecules22111894.

Chuyen, H.V., Eun, J.B., 2017. Marine carotenoids: Bioactivities and potential benefits to human health. Crit. Rev. Food Sci. Nutr. 57, 2600–2610.

Dahmoune, F., Spigno, G., Moussi, K., Remini, H., Cherbal, A., Madani, K., 2014. *Pistacia lentiscus* leaves as a source of phenolic compounds: microwave-assisted extraction optimized and compared with ultrasound-assisted and conventional solvent extraction. Ind. Crops Prod. 61, 31–40. https://doi.org/10.1080/10408398.2015.1063477.

Dean, A.P., Estrada, B., Sigee, D.C., 2010. Pittman JK Using FTIR spectroscopy for rapid determination of lipid accumulation in response to nitrogen limitation in freshwater microalgae. Bioresour. Technol. 101, 4499–4507. https://doi.org/10.1016/j.biortech.2010.01.065.

Del Campo, J.A., Morenom, J., Rodríguezm, H., Vargasm, M.A., Rivasm, J., Guerrero, M.G., 2000. Carotenoid content of chlorophycean microalgae. Factors determining lutein accumulation in *Muriellopsis sp.* (Chlorophyta). J. Biotechnol. 76, 51–59. https://doi.org/10.1016/s0168-1656(99)00178-9.

Fimbres-Olivarría, D., López-Elías, J.A., Martínez-Córdova, L.R., Carvajal-Millán, E., Enríquez-Ocaña, F., Valdéz-Holguín, E., Miranda-Baeza, A., 2015. Growth and Biochemical Composition of *Navicula sp*. Cultivated at Two Light Intensities and Three Wavelengths. Isr. J. Aquacult-Bamid 67, 1155.

Fimbres-Olivarría, D. et al., 2016. *Navicula* sp. Sulfated Polysaccharide Gels Induced by Fe (III): Rheology and Microstructure. Int. J. Molecul. Sci. 17, 1238.

Finkel, T., Holbrook, N.J., 2000. Oxidants, oxidative stress and the biology of ageing. Nature 408, 239–247. https://doi.org/10.1038/35041687.

Fratoddi, I., Rapa, M., Testa, G., Venditti, I., Scaramuzzo, F.A., Vinci, G., 2018. Response surface methodology for the optimization of phenolic compounds extraction from extra virgin olive oil with functionalized gold nanoparticles. Microchem. J. 138, 430–437. https://doi.org/10.1016/j.microc.2018.01.043.

Fu, W., Wichuk, K., Brynjólfsson, S., 2015. Developing diatoms for value-added products: challenges and opportunities. New Biotech. J. 32, 547–551.

Gagez, A.L., Thiéry, V., Pasquet, V., Cadoret, J.P., Picot, L., 2012. Epoxycarotenoids and cancer. Curr. Bioact. Compd. 8, 109–141. https://doi.org/10.1016/j.nbt.2015.03.016.

García-Morales, J., López-Elías, J.A., Medina-Félix, D., García-Lagunas, N., Fimbres-Olivarría, D., 2020. Effect of nitrogen and salinity stress on the β-carotene content of the microalgae Dunaliella tertiolecta. Biotecnia. 22 (2), 13–19. https://doi.org/10.18633/biotecnia.v22i2.1241.

Goiris, K., Van Colen, W., Wilches, I., León Tamariz, F., De Cooman, L., Muylaert, K., 2015. Impact of nutrient stress on antioxidant production in three species of microalgae. Algal Research. 7, 51–57. https://doi.org/10.1016/j.algal.2014.12.002.

Gonçalves, C.F., Menegol, T., Rech, R., 2019. Biochemical composition of green microalgae *Pseudoneochloris marina* grown under different temperature and light conditions. Biocatal. Agricult. Biotechnol. 18,. https://doi.org/10.1016/j.bcab.2019.101032 101032.

Gong, M., Bassi, A., 2016. Carotenoids from microalgae: a review of recent developments. Biotechnol. Adv. 34, 1396–1412. https://doi.org/10.1016/j.biotechadv.2016.10.005.

Guillard, R.L., Ryther, J.H., 1962. Studies on marine planktonic diatoms I. *Cyclotella nana* Husted and Detonula confervacea (Cleve) Gran. Can. J. Microbiol. 8, 229–239. https://doi.org/10.1139/m62-029.

Hajimahmoodi, M., Faramarzi, M.A., Mohammadi, N., Soltani, N., Oveisi, M.R., Nafissi-Varamarzi, N., 2010. Evaluation of antioxidant properties and total phenolic contents of some strains microalgae. J. Appl. Phycol. 22, 43–50. https://doi.org/10.1007/s10811-009-9424-y.

Hanrahan, G., Lu, K., 2006. Application of Factorial and Response Surface Methodology in Modern Experimental Design and Optimization. Crit. Rev. Anal. Chem. 36 (3–4), 141–151. https://doi.org/10.1080/10408340600969478.

Hu, J., Nagarajan, D., Zhang, Q., Chang, J.S., Lee, D.J., 2018. Heterotrophic cultivation of microalgae for pigment production: A review. Biotechnol. Adv. 36 (1), 54–67. https://doi.org/10.1016/j.biotechadv.2017.09.009.

Imamoglu, E., Dalay, M.C., Sukan, F.V., 2009. Influence of different stress media and high light intensities on accumulation of astaxanthin in green alga *Haematococcus pluvialis*. New Biotechnol. 26, 199–204. https://doi.org/10.1016/j.nbt.2009.08.007.

Jeffrey, S.W., Humphrey, G.F., 1975. New Spectrophotometric Equations for Determining Chlorophylls *a, b* c_1 *and* c_2 in Higher Plants, Algae and Natural Phytoplankton. Biochem. Physiol. Pflanz. (BPP) 167, 191–194. https://doi.org/10.1016/S0015-3796(17)30778-3.

Kooijman, E.E., Chupin, V., Fuller, N.L., Kozlov, M.M., Kruijff, B., Burger, K.N., Rand, P. R., 2005. Spontaneous curvature of phosphatidic acid and lysophosphatidic acid. Biochem. 44, 2097–2102. https://doi.org/10.1021/bi0478502.

Kraʙs, G., Buʗchel, C., 2011. Temperature and salinity tolerances of geographically separated *Phaeodactylum tricornutum* Boʜlin strains: maximum quantum yield of primary photochemistry, pigmentation, proline content and growth. Bot. Mar. 54, 231–241. https://doi.org/10.1515/bot.2011.037.

Krell, A, Funcke, D, Plettner, I, John, U, Dieckmann, G, 2007. Regulation of proline metabolism under salt stress in the psychrophilic diatom *fragilariopsis cylindrus* (Bacillariophyceae). J. Phycol. 43, 753–762. https://doi.org/10.1111/j.1529-8817.2007.00366.x.

Kumar, M, Kumari, P, Gupta, V, Reddy, C.R.K, Jha, B, 2010. Biochemical responses of red alga *Gracilaria corticata* (Gracilariales, Rhodophyta) to salinity induced oxidative stress. J. Exp. Mar. Biol. Ecol. 391, 27–34. https://doi.org/10.1016/j.jembe.2010.06.001.

Kyong-Hwa, K., Zhong-Ji, Q., BoMi, R., Se-Kwon, K., 2011. Characterization of growth and protein contents from microalgae *Navicula incerta* with the investigation of antioxidant activity of enzymatic hydrolysates. Food Sci. Biotechnol. 20 (1), 183–191. https://doi.org/10.1007/s10068-011-0025-6.

Laokuldilok, N., Thakeow, P., Kopermsub, P., Utama-ang, N., 2016. Optimizations of microencapsulation of turmeric extract for masking flavor. Food Chem. 194, 695–704. https://doi.org/10.13140/RG.2.1.2788.1443.

Lee, J.B., Hayashi, K., Hirata, M., Kuroda, E., Suzuki, E., Kubo, Y., Hayashi, T., 2006. Antiviral sulfated polysaccharide from *Navicula directa*, a diatom collected from deep-sea water in Toyama Bay. Biol. Pharm. Bull. 29, 2135–2139. https://doi.org/10.1248/bpb.29.2135.

Lefsih, K. et al., 2017. Pectin from *Opuntia ficus indica*: optimization of microwave-assisted extraction and preliminary characterization. Food Chem. 221, 91–99. https://doi.org/10.1016/j.foodchem.2016.10.073.

Lewin, J., Lewin, R., 1960. Auxotrophy and heterotrophy in marine littoral diatoms. Can. J. Microbiol. 6, 127–134. https://doi.org/10.1139/m60-015.

Li, Y., Horsman, M., Wang, B., Wu, N., Lan, C.Q., 2008. Effects of nitrogen sources on cell growth and lipid accumulation of green alga *Neochloris oleoabundans*. Appl. Microbiol. Biotechnol. 81, 629–636. https://doi.org/10.1007/s00253-008-1681-1.

Li, Y., Li, S., Lin, S.J., Zhang, J.J., Zhao, C.N., Li, H.B., 2017. Microwave-assisted extraction of natural antioxidants from the exotic *Gordonia axillaris* fruit: Optimization and identification of phenolic compounds. Molecules 22, 1481. https://doi.org/10.3390/molecules22091481.

Liang, Y., Sun, M., Tian, C., Cao, C., Li, Z., 2014. Effects of salinity stress on the growth and chlorophyll fluorescence of *Phaeodactylum tricornutum* and *Chaetoceros gracilis* (Bacillariophyceae). Bot. Mar. 57 (6), 469–476. https://doi.org/10.1515/bot-2014-0037.

Lichtendthaler & Welburn. 1983. Determinations of total carotenoids and chlorophylls a and b of leaf extracts in different solvents. Botanisches Institut der Universitat, KaiserstraJe 12). Department of Biological Sciences, UniversityofLancaster, Bailrigg, Lancaster LA1 4YQ, UX.

Liu, R.H., Finley, J., 2005. Potential cell culture models for antioxidant research. J. Agricul. Food Chem. 53, 4311–4314. https://doi.org/10.1021/jf058070i.

Liu, S., Huang, H., 2015. Assessments of antioxidant effect of black tea extract and its rationals by erythrocyte haemolysis assay, plasma oxidation assay and cellular antioxidant activity (CAA) assay. J. funct. foods. 18, 1095–1105. https://doi.org/10.1016/j.jff.2014.08.023.

López-Elías, J.A., Fimbres-Olivarría, D., Medina-Juárez, L.A., Miranda-Baeza, A., Martínez-Córdova, L.R., Molina-Quijada, D.M.A., 2013. Production of biomass and carotenoids of Dunaliella tertiolecta in nitrogen-limited cultures. Phyton. 82, 23–30 https://www.researchgate.net/publication/260750162_Production_of_biomass_and_carotenoids_of_Dunaliella_tertiolecta_in_nitrogen-limited_cultures.

Lourenço, S.O., Barbarino, E., Lavín, P.L., Marquez, U.M.L., Aidar, E., 2004. Distribution of intracellular nitrogen in marine microalgae: calculation of new nitrogen-to-protein conversion factors. Eur. J. Phycol. 39, 17–32. https://doi.org/10.1080/0967026032000157156.

Lu, C., Zhang, J., 2000. Role of light in the response of PSII photochemistry to salt stress in the cyanobacterium *Spirulina platensis*. J. Exp. Bot. 51, 911–917. https://doi.org/10.1093/jxb/51.346.911.

Lu, C., Vonshak, A., 2002. Effects of salinity stress on photosystem II function in cyanobacterial *Spirulina platensis* cells. Physiol. Plant. 114, 405–413 http://www.bashanfoundation.org/contributions/Vonshak-A/vonshaksalinystress.pdf.

Lu, J. et al., 2010. Flavonoids from the leaves of *Actinidia kolomikta*. Chem. Nat. Compd. 46, 205–208 https://link.springer.com/article/10.1007/s10600-010-9569-6.

Markou, G., Angelidaki, I., Georgakakis, D., 2012. Microalgal carbohydrates: an overview of the factors influencing carbohydrates production, and of main bioconversion technologies for production of biofuels. Mini Review. Appl. Microbiol. Biotechnol. 96, 631–645. https://doi.org/10.1007/s00253-012-4398-0.

Markou, G., Nerantzis, E., 2013. Microalgae for high-value compounds and biofuels production: a review with focus on cultivation under stress conditions. Biotechnol. Adv. 8, 1532–1542. https://doi.org/10.1016/j.biotechadv.2013.07.011.

Masojídek, J., Torzillo, G., Kopeck, J., KoblíÊek, M., Nidiaci, L., Komenda, J., Lukavská, A., Sacchi, A., 2000. Changes in chlorophyll fluorescence quenching and pigment composition in the green alga *Chlorococcum* sp. grown under nitrogen deficiency and salinity stress. J. Appl. Phycol. 12, 417–426 https://link.springer.com/article/10.1023%2FA%3A1008165900780.

Muller Feuga, A., Moal, J., Kaas, R., 2007. The microalgae of aquaculture. In: Live feeds in marine aquaculture (ed. Støttrup JG, McEvoy LA). Blackwell Sci 1, 207–252.

Mustafa, T. et al., 2019. Variation in growth, fucoxanthin, fatty acids profile and lipid content of marine diatoms *Nitzschia* sp. and *Nanofrustulum shiloi* in response to nitrogen and iron. Biocatal. Agricul. Biotechnol. 17, 390–398. https://doi.org/10.1016/j.bcab.2018.12.023.

Myers, R.H., Montgomery, D.C., Anderson-Cook, C.M., 2009. "The analysis of second-order response surfaces," in Response Surface Methodology. Process and Product Optimization Using Designed Experiments. John Wiley & Sons Hoboken NJ USA 3rd edition.

Prior, R.L., Wu, X., Schaich, K., 2005. Standardized methods for the determination antioxidant capacity and phenolics in foods and dietary supplements. J. Agricult. Food Chem. 53, 4290–4302. https://doi.org/10.1021/jf0502698.

Radchenko, I.G, Il'yash, L.V, 2006. Growth and photosynthetic activity of diatom *Thalassiosira weissflogii* at decreasing salinity. Plant Physiol. 33 (3), 242–247.

Re, R., Pellegrini, N., Proteggente, A., Pannala, A., Yang, M., Rice-Evans, C., 1999. Antioxidant activity applying an improved ABTS radical cation decolorization assay. Free Rad. Biol. Med. 10, 1231–1237. https://doi.org/10.1016/S0891-5849(98)00315-3.

Richmond, A., 2004. Biological principles of mass cultivation, in: A. Richmond (Ed.), Handbook of Microalgal Mass Culture: Blackwell Oxford. Biotechnol. Appl. Phycol. Blackwell Sci. 1, 147-239.

Rijstenbil, J.W., 2005. UV- and salinity-induced oxidative effects in the marine diatom *Cylindrotheca closterium* during simulated emersion. Mar. Biol. 147, 1063–1073. https://doi.org/10.1007/s00227-005-0015-4.

Sánchez Saavedra, M.P., Núñez, Z., 2012. Photosynthetic and biochemical effects of cold storage on marine benthic diatoms of the Mexican pacific coast. J. World Aquacult Soc. 43 (2), 249–258. https://doi.org/10.1111/j.1749-7345.2012.00553.x.

Saranya, C., Hemalatha, A., Parthiban, C., Anantharaman, P., 2014. Evaluation of Antioxidant Properties, Total Phenolic and Carotenoid Content of *Chaetoceros calcitrans*, *Chlorella salina* and *Isochrysis galbana*. Int. J. Curr. Microbiol. App. Sci. 3 (8), 365–377 https://www.ijcmas.com/vol-3-8/C.Saranya,%20et%20al.pdf.

Saurabh, C.K., Gupta, S., Variyar, P.S., Sharma, A., 2016. Effect of addition of nanoclay, beeswax, tween-80 and glycerol on physicochemical properties of guar gum films. Ind. Crops Prod. 89, 109–118. https://doi.org/10.1016/j.indcrop.2016.05.003.

Schubert, H., Fulda, S., Hagemann, M., 1993. Effects of adaptation to different salt concentrations on photosynthesis and pigmentation of the cyanobacterium *Synechocystis* sp. P.C.C. 6803. J. Plant Physiol. 142, 291–295. https://doi.org/10.1016/S0176-1617(11)80425-6.

Sorokin, C., 1973. Dry weight, packed volume and optical density. Handbook of Physiological Methods. Culture Methods and Growth Measurement. Cambridge University, Press, Cambridge, p. 448.

St. John, M.A., Clemmesen, C., Lund, T., Köster, T., 2001. Diatom production in the marine environment: Implications for larval fish growth and condition. ICES J. Mar. Sci. 58, 1106–1113. https://doi.org/10.1006/jmsc.2001.1089.

Tibbetts, S.M., Milley, J.E., Lall, S.P., 2014. Chemical composition and nutritional properties of freshwater and marine microalgal biomass cultured in photobioreactors. J. Appl. Phycol. https://doi.org/10.1007/s10811-014-0428-x.

Touchette, B.W., Burkholder, J.M., 2000. Review of nitrogen and phosphorus metabolism in seagrasses. J. Exp. Mar. Bio. Ecol. 250, 133–167. https://doi.org/10.1016/S0022-0981(00)00195-7.

Wai Kuan, Y., 2019. Metabolic and physiological regulation of *Chlorella* sp. (Trebouxiophyceae, Chlorophyta) under nitrogen deprivation. J. Oceanol. Limnol. 37, 186–198. https://doi.org/10.1007/s00343-019-7263-5.

Wang, X., Fosse, H.K., Li, K., Chauton, M.S., Vadstein, O., Reitan, K.I., 2019. Influence of Nitrogen Limitation on Lipid Accumulation and EPA and DHA Content in Four Marine Microalgae for Possible Use in Aquafeed. Front. Mar. Sci. 6, 95. https://doi.org/10.3389/fmars.2019.00095.

Widowati, I., Zainuri, M., Kusumaningrum, H.P., Susilowati, R., Hardivillier, Y., Leignel, V., Bourgougnon, N., Mouget, J., 2017. Antioxidant activity of three microalgae *Dunaliella salina, Tetraselmis chuii* and *Isochrysis galbana* clone Tahiti. IOP Conf Ser: Earth Environ. Sci. 55,. https://doi.org/10.1088/1755-1315/55/1/012067 012067.

Xin, L., Hu, H.Y., Ke, G., Sun, Y.X., 2010. Effects of different nitrogen and phosphorus concentrations on the growth, nutrient uptake, and lipid accumulation of a freshwater microalga *Scenedesmus* sp. Bioresour. Technol. 101 (14), 5494–5500. https://doi.org/10.1016/j.biortech.2010.02.016.

Yancey, P.H., 2005. Organic osmolytes as compatible, metabolic, and counteracting cytoprotectants in high osmolarity and other stresses. J. Exp. Biol. 208, 2819–2830. https://doi.org/10.1242/jeb.01730.